

NNLO vertex corrections in charmless hadronic B decays: Real part

GUIDO BELL¹

*Institut für Theoretische Teilchenphysik,
Universität Karlsruhe, D-76128 Karlsruhe, Germany*

Abstract

We compute the real part of the 2-loop vertex corrections for charmless hadronic B decays, completing the NNLO calculation of the topological tree amplitudes in QCD factorization. Among the technical aspects we show that the hard-scattering kernels are free of soft and collinear infrared divergences at the 2-loop level, which follows after an intricate subtraction procedure involving evanescent four quark operators. The numerical impact of the considered corrections is found to be moderate, whereas the factorization scale dependence of the topological tree amplitudes is significantly reduced at NNLO. We in particular do not find an enhancement of the phenomenologically important ratio $|C/T|$ from the perturbative calculation.

¹E-mail: bell@particle.uni-karlsruhe.de

1 Introduction

The study of hadronic B meson decays into a pair of light (charmless) mesons reveals interesting information about the underlying four quark interactions and the related phenomenon of CP violation. While these decay modes are intensively investigated at current and future B physics experiments, the main challenge for precise theoretical predictions consists in the computation of the hadronic matrix elements. QCD factorization [1], or its field theoretical formulation in the language of Soft-Collinear Effective Theory [2], is a systematic framework to compute these matrix elements from first principles. The starting point is a factorization formula, which holds in the heavy quark limit $m_b \rightarrow \infty$,

$$\begin{aligned} \langle M_1 M_2 | Q_i | \bar{B} \rangle \simeq & F_+^{BM_1}(0) f_{M_2} \int du \, T_i^I(u) \phi_{M_2}(u) \\ & + \hat{f}_B f_{M_1} f_{M_2} \int d\omega dv du \, T_i^{II}(\omega, v, u) \phi_B(\omega) \phi_{M_1}(v) \phi_{M_2}(u), \end{aligned} \quad (1)$$

where the perturbatively calculable hard-scattering kernels $T_i^{I,II}$ encode the short-distance strong-interaction effects and the non-perturbative physics is confined to some process-independent hadronic parameters such as decay constants f_M , light-cone distribution amplitudes ϕ_M and a transition form factor $F_+^{BM_1}$ at maximum recoil $q^2 = 0$.

In this work we address perturbative corrections to the factorization formula (1). Whereas next-to-leading order (NLO) corrections to the hard-scattering kernels $T_i^{I,II}$ are known from the pioneering work in [1], partial next-to-next-to-leading order (NNLO) corrections have recently been worked out [3, 4, 5, 6]. The α_s^2 corrections to the kernels T_i^{II} (*spectator scattering*) are by now completely determined to NNLO: the corrections for the topological tree amplitudes have been computed in [3] and the ones for the so-called penguin amplitudes in [4].

In contrast to this the computation of α_s^2 corrections to the kernels T_i^I (*vertex corrections*) is to date incomplete. Whereas we computed the imaginary parts of the hard-scattering kernels for the topological tree amplitudes in [5, 6], we complete the NNLO calculation of the tree amplitudes in this work by computing the respective real parts. Partial results of this calculation, in particular the analytical expressions of the required 2-loop Master Integrals, have already been given in [6].

The organization of this paper is as follows: The technical aspects of the NNLO calculation are presented in Section 2. We start by briefly recalling our definitions and conventions and make some remarks concerning the computation of the 2-loop diagrams. We then show in some detail how to extract the hard-scattering kernels from the matrix elements which are formally infrared divergent. This subtraction procedure, which becomes particularly involved for the colour-suppressed tree amplitude, is complicated due to the presence of evanescent four quark operators which arise in intermediate steps of the calculation. Our analytical results for the hard-scattering kernels are summarized in Section 3. We briefly discuss the numerical impact of the considered NNLO corrections in Section 4, before we conclude in Section 5. Several technical issues of the calculation and the explicit expressions of the hard-scattering kernels are relegated to the Appendix.

2 NNLO calculation

The calculation of the real parts of the topological tree amplitudes proceeds along the same lines as the one of the imaginary parts that we presented in [5]. Still, the current calculation turns out to be considerably more complex in several respects. First, it requires the calculation of a larger amount of 2-loop integrals, which are in addition more complicated since they involve up to three (instead of one) massive propagators. Second, the renormalization procedure and the infrared subtractions reveal their full 2-loop complexity only in the current calculation as a consequence of the fact that the tree level contribution is real. In the following we summarize the technical aspects of the calculation and refer for a more detailed description of the general strategy to [5] (cf. also [6]).

2.1 Operator basis

The topological tree amplitudes can be derived from the hadronic matrix elements of the current-current operators in the effective weak Hamiltonian

$$\mathcal{H}_{\text{eff}} = \frac{G_F}{\sqrt{2}} V_{ud}^* V_{ub} (C_1 Q_1 + C_2 Q_2) + \text{h.c.} \quad (2)$$

As we apply Dimensional Regularization¹ (DR) to regularize ultraviolet (UV) and infrared (IR) singularities, evanescent four-quark operators appear in intermediate steps of the calculation. The full operator basis required for the present calculation becomes²

$$\begin{aligned} Q_1 &= [\bar{u}\gamma^\mu L T^A b] [\bar{d}\gamma_\mu L T^A u], \\ Q_2 &= [\bar{u}\gamma^\mu L b] [\bar{d}\gamma_\mu L u], \\ E_1 &= [\bar{u}\gamma^\mu \gamma^\nu \gamma^\rho L T^A b] [\bar{d}\gamma_\mu \gamma_\nu \gamma_\rho L T^A u] - 16 Q_1, \\ E_2 &= [\bar{u}\gamma^\mu \gamma^\nu \gamma^\rho L b] [\bar{d}\gamma_\mu \gamma_\nu \gamma_\rho L u] - 16 Q_2, \\ E'_1 &= [\bar{u}\gamma^\mu \gamma^\nu \gamma^\rho \gamma^\sigma \gamma^\tau L T^A b] [\bar{d}\gamma_\mu \gamma_\nu \gamma_\rho \gamma_\sigma \gamma_\tau L T^A u] - 20 E_1 - 256 Q_1, \\ E'_2 &= [\bar{u}\gamma^\mu \gamma^\nu \gamma^\rho \gamma^\sigma \gamma^\tau L b] [\bar{d}\gamma_\mu \gamma_\nu \gamma_\rho \gamma_\sigma \gamma_\tau L u] - 20 E_2 - 256 Q_2, \end{aligned} \quad (3)$$

with colour matrices T^A and $L = 1 - \gamma_5$. We stress that previous studies within QCD factorization, as e.g. [1, 3, 4], have often been formulated in a different operator basis with a Fierz-symmetric definition of the physical operators. As has been argued in [5], it is more convenient for the current calculation to use the operator basis (3) since it allows to work with a naive anticommuting γ_5 beyond NLO [7].

There are two different insertions of a four-quark operator which are illustrated in Figure 1 of [5]. The first one gives rise to the colour-allowed tree amplitude $\alpha_1(M_1 M_2)$, which corresponds to the flavour content $[\bar{q}_s b]$ of the decaying \bar{B} meson, $[\bar{q}_s u]$ of the recoil

¹We write $d = 4 - 2\epsilon$ and use an anticommuting γ_5 according to the NDR scheme.

²This operator basis has been named *CMM basis* in [5] (denoted by a hat).

meson M_1 and $[\bar{u}d]$ of the emitted meson M_2 . The colour-suppressed tree amplitude $\alpha_2(M_1 M_2)$ follows from the second insertion and belongs to the flavour contents $[\bar{q}_s b]$, $[\bar{q}_s d]$ and $[\bar{u}u]$, respectively. In [5] we did not consider the second type of insertions since we could derive the imaginary part of the colour-suppressed amplitude from the one of the colour-allowed amplitude using Fierz-symmetry arguments³.

In the current calculation we cannot proceed along the same lines, since a Fierz-symmetric operator basis has not yet been worked out to NNLO⁴. We therefore consider both types of insertions in this work, which also provides an independent cross-check of our previous result for the imaginary part of the colour-suppressed tree amplitude.

2.2 2-loop calculation

The main task of the calculation consists in the computation of a large number of 2-loop diagrams (shown in Figure 2 of [5]). We use an automatized reduction algorithm, which is based on integration-by-parts techniques [11], to express these diagrams in terms of an irreducible set of Master Integrals (MIs). In addition to the MIs that appeared in the calculation of the imaginary part of the NNLO vertex corrections (cf. Figure 3 of [5]), we find 22 MIs which are shown in Figure 1. In total the current calculation requires the computation of 36 MIs to up to five orders in the ε -expansion.

Apart from the MIs that involve the charm quark mass, the analytical results for the MIs from Figure 1 can be found in [6]⁵. The MIs can be expressed in terms of Harmonic Polylogarithms (HPLs) [14] of weight $w \leq 4$,

$$\begin{aligned}
H(0; x) &= \ln(x), & H(0, 0, 1; x) &= \text{Li}_3(x), \\
H(1; x) &= -\ln(1-x), & H(0, 1, 1; x) &= \text{S}_{1,2}(x), \\
H(-1; x) &= \ln(1+x), & H(0, 0, 0, 1; x) &= \text{Li}_4(x), \\
H(0, 1; x) &= \text{Li}_2(x), & H(0, 0, 1, 1; x) &= \text{S}_{2,2}(x), \\
H(0, -1; x) &= -\text{Li}_2(-x), & H(0, 1, 1, 1; x) &= \text{S}_{1,3}(x). \\
H(-1, 0, 1; x) &\equiv \mathcal{H}_1(x), & H(0, -1, 0, 1; x) &\equiv \mathcal{H}_2(x),
\end{aligned} \tag{4}$$

where we introduced a shorthand notation for the last two HPLs⁶. Moreover, the massive non-planar 6-topology MI (last diagram from Figure 1) involves a constant in the finite term which, until recently, was only known numerically, $\mathcal{C}_0 = -60.2493267(10)$ [13]. In a recent work it was shown that its analytical value is $\mathcal{C}_0 = -167\pi^4/270$ [16].

³To do so we introduced a second operator basis named *traditional basis* in [5] (denoted by a tilde).

⁴We emphasize that the operator basis from Section 8 in [8] is not Fierz-symmetric and the one from Appendix A in [9] is presumably not either [10].

⁵Part of these results have recently been confirmed by various groups [12, 13].

⁶The explicit expression of $\mathcal{H}_1(x)$ in terms of Nielsen Polylogarithms can be found e.g. in equation (10) of [15]. On the other hand $\mathcal{H}_2(x)$ has to be evaluated numerically (in Section 3.2 we find, however, analytical expressions in the convolutions with the light-cone distribution amplitude of the meson M_2).

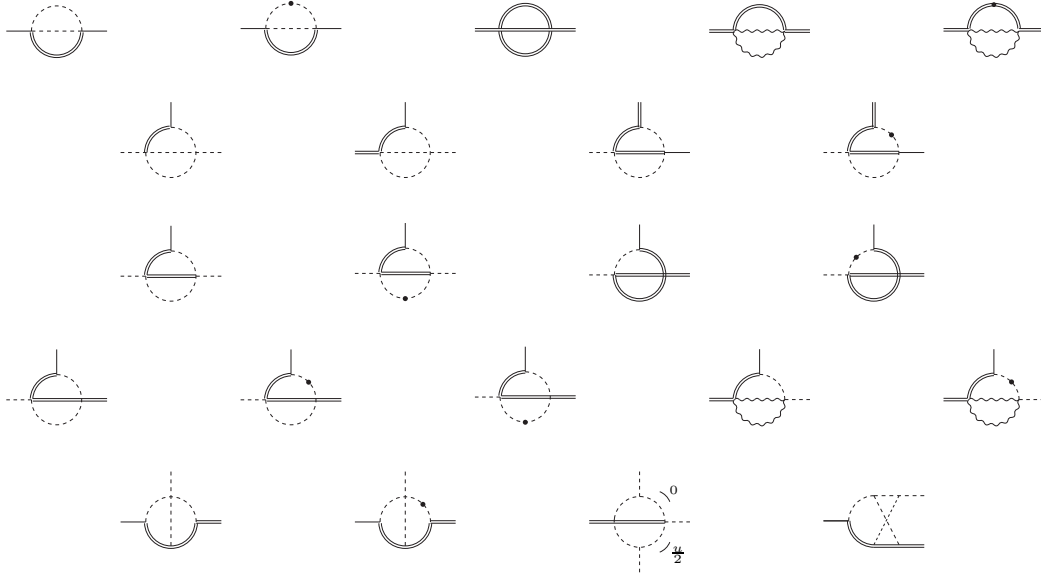


Figure 1: *Additional Master Integrals that appear in the calculation of the real parts of the NNLO vertex corrections. Dashed/double/wavy internal lines denote propagators with mass 0 / m_b / m_c . Dashed/solid/double external lines correspond to virtualities 0 / um_b^2 / m_b^2 . Dotted propagators are taken to be squared.*

The charm mass dependent MIs can be found in [6, 15]. In this case there exist analytical results apart from the finite terms of two 4-topology MIs. We may, however, evaluate these contributions numerically to implement charm mass effects in the current analysis.

2.3 Renormalization

The calculation of the renormalized matrix elements requires standard counterterms from QCD and the effective Hamiltonian. We write the renormalized matrix elements as

$$\langle Q_i \rangle = Z_\psi Z_{ij} \langle Q_j \rangle_{\text{bare}}, \quad (5)$$

where Z_ψ contains the wave-function renormalization factors of the quark fields and Z is the operator renormalization matrix in the effective theory. Here and below we introduce a shorthand notation for the perturbative expansions,

$$\langle Q_i \rangle_{(\text{bare})} = \sum_{k=0}^{\infty} \left(\frac{\alpha_s}{4\pi} \right)^k \langle Q_i \rangle_{(\text{bare})}^{(k)}, \quad Z_{ij} = \delta_{ij} + \sum_{k=1}^{\infty} \left(\frac{\alpha_s}{4\pi} \right)^k Z_{ij}^{(k)}. \quad (6)$$

It turns out that the wave-function renormalization factors in Z_ψ can be neglected in the calculation of the hard-scattering kernels since they are absorbed by the form factor and the light-cone distribution amplitude in the factorization formula, which are defined in

terms of full QCD fields (rather than HQET or SCET fields), for details cf. Section 4.2 of [5]. We renormalize the coupling constant in the $\overline{\text{MS}}$ -scheme,

$$Z_g^{(1)} = - \left(\frac{11}{6} C_A - \frac{1}{3} n_f \right) \frac{1}{\varepsilon}, \quad (7)$$

and the b -quark mass in the on-shell scheme,

$$Z_m^{(1)} = -C_F \left(\frac{e^{\gamma_E} \mu^2}{m_b^2} \right)^\varepsilon \Gamma(\varepsilon) \frac{3 - 2\varepsilon}{1 - 2\varepsilon}. \quad (8)$$

The 1-loop and 2-loop $\overline{\text{MS}}$ operator renormalization matrices can be inferred from [8, 17]

$$\begin{aligned} Z^{(1)} &= \begin{pmatrix} -2 & \frac{4}{3} & \frac{5}{12} & \frac{2}{9} & 0 & 0 \\ 6 & 0 & 1 & 0 & 0 & 0 \end{pmatrix} \frac{1}{\varepsilon}, \\ Z^{(2)} &= \begin{pmatrix} 17 - \frac{2}{3}n_f & -\frac{26}{3} + \frac{4}{9}n_f & -\frac{25}{6} + \frac{5}{36}n_f & -\frac{31}{18} + \frac{2}{27}n_f & \frac{19}{96} & \frac{5}{108} \\ -39 + 2n_f & 4 & -\frac{31}{4} + \frac{1}{3}n_f & 0 & \frac{5}{24} & \frac{1}{9} \end{pmatrix} \frac{1}{\varepsilon^2} \\ &+ \begin{pmatrix} \frac{79}{12} + \frac{4}{9}n_f & -\frac{205}{18} + \frac{10}{27}n_f & \frac{1531}{288} - \frac{5}{216}n_f & -\frac{1}{72} - \frac{1}{81}n_f & \frac{1}{384} & -\frac{35}{864} \\ \frac{83}{4} + \frac{5}{3}n_f & 3 & \frac{119}{16} - \frac{1}{18}n_f & \frac{8}{9} & -\frac{35}{192} & -\frac{7}{72} \end{pmatrix} \frac{1}{\varepsilon}, \quad (9) \end{aligned}$$

where the lines refer to the physical operators and the columns to the full operator basis including the evanescent operators from (3).

2.4 IR subtractions

In order to extract the hard-scattering kernels T_i we rewrite the renormalized matrix elements in the factorized form

$$\langle Q_i \rangle = F \cdot T_i \otimes \Phi + \dots \quad (10)$$

where F denotes the form factor, Φ the product of decay constant and distribution amplitude, \otimes the convolution integral and the ellipsis the spectator scattering term which we disregard in the following. As has been discussed in detail in Section 4.2 of [5], only naively non-factorizable (nf) 1-loop diagrams contribute to the NLO kernels,

$$\langle Q_i \rangle_{\text{nf}}^{(1)} + Z_{ij}^{(1)} \langle Q_j \rangle^{(0)} = F^{(0)} \cdot T_i^{(1)} \otimes \Phi^{(0)}. \quad (11)$$

Similarly, the calculation of the NNLO kernels involves only non-factorizable 2-loop diagrams (but factorizable (f) 1-loop diagrams),

$$\begin{aligned} \langle Q_i \rangle_{\text{nf}}^{(2)} + Z_{ij}^{(1)} \left[\langle Q_j \rangle_{\text{nf}}^{(1)} + \langle Q_j \rangle_{\text{f}}^{(1)} \right] + Z_{ij}^{(2)} \langle Q_j \rangle^{(0)} \\ = F^{(0)} \cdot T_i^{(2)} \otimes \Phi^{(0)} + F_{\text{amp}}^{(1)} \cdot T_i^{(1)} \otimes \Phi^{(0)} + F^{(0)} \cdot T_i^{(1)} \otimes \Phi_{\text{amp}}^{(1)}, \quad (12) \end{aligned}$$

where the subscript "amp" (amputated) has been introduced to denote corrections without wave-function renormalization. We see that the calculation of the NNLO kernels requires the NLO kernels to $\mathcal{O}(\varepsilon^2)$ as they enter (12) in combination with the IR-divergent form factor correction $F_{\text{amp}}^{(1)} \sim 1/\varepsilon_{\text{IR}}^2$. As a consequence the factorization formula has to be extended in intermediate steps of the calculation to include evanescent operators, which have to be renormalized such that their (IR-finite) matrix elements vanish (for details cf. Section 4.3 of [5]).

At NNLO the subtraction procedure becomes somewhat involved. It is particularly complicated in the calculation of the colour-suppressed tree amplitude, where a Fierz-evanescent operator appears at tree level. In the following we discuss the subtraction procedure in some detail. Throughout this section we concentrate on the real parts of the hard-scattering kernels, since the respective imaginary parts have already been given in [5]. We refer to Appendix A for the explicit expressions of the auxiliary coefficient functions $t_i(u)$ that we introduce below.

Colour-allowed tree amplitude

To NNLO we find three operators that contribute to the right hand side of (10). In the position space representation they correspond to products of a local heavy-to-light current $\bar{u}(x)\Gamma_1 b(x)$ and a non-local light-quark current $\bar{d}(y)[y, x]\Gamma_2 u(x)$, where the usual gauge link factor $[y, x]$ is understood. We choose the basis of Dirac structures $\Gamma_1 \otimes \Gamma_2$ as⁷

$$\begin{aligned}\mathcal{O} &= [\gamma^\mu L] \otimes [\gamma_\mu L], \\ \mathcal{O}_E &= [\gamma^\mu \gamma^\nu \gamma^\rho L] \otimes [\gamma_\mu \gamma_\nu \gamma_\rho L] - 16 \mathcal{O}, \\ \mathcal{O}_{E'} &= [\gamma^\mu \gamma^\nu \gamma^\rho \gamma^\sigma \gamma^\tau L] \otimes [\gamma_\mu \gamma_\nu \gamma_\rho \gamma_\sigma \gamma_\tau L] - 20 \mathcal{O}_E - 256 \mathcal{O},\end{aligned}\tag{13}$$

such that the factorized hadronic matrix element of \mathcal{O} gives the standard QCD form factor and the light-cone distribution amplitude of the emitted meson M_2 . The operators \mathcal{O}_E and $\mathcal{O}_{E'}$ are evanescent.

We first compute (11) to $\mathcal{O}(\varepsilon^2)$ to determine the NLO kernels. We find that the colour-singlet kernels vanish, $T_2^{(1)} = T_{2,E}^{(1)} = T_{2,E'}^{(1)} = 0$, while the colour-octet kernels become

$$\begin{aligned}\text{Re } T_1^{(1)}(u) &= \frac{C_F}{2N_c} \left(\frac{\mu^2}{m_b^2} \right)^\varepsilon \left\{ t_0(u) - 6L + \left(t_1(u) + 3L^2 \right) \varepsilon + \left(t_2(u) - L^3 \right) \varepsilon^2 + \mathcal{O}(\varepsilon^3) \right\}, \\ \text{Re } T_{1,E}^{(1)}(u) &= -\frac{C_F}{4N_c} \left(\frac{\mu^2}{m_b^2} \right)^\varepsilon \left\{ t_{E,0}(u) + 2L + \left(t_{E,1}(u) - L^2 \right) \varepsilon + \mathcal{O}(\varepsilon^2) \right\},\end{aligned}\tag{14}$$

and $T_{1,E'}^{(1)} = 0$ with $L = \ln \mu^2/m_b^2$. The IR subtractions on the right hand side of (12) require in addition form factor and wave function corrections to the operators \mathcal{O} and \mathcal{O}_E (they can be found in Section 4.3 of [5]). We finally perform the convolutions of the NLO

⁷We do not consider colour-octet operators since their hadronic matrix elements vanish.

kernels with the wave function corrections, which yields

$$F^{(0)} \text{Re } T_1^{(1)} \Phi_{\text{amp}}^{(1)} = \frac{C_F^2}{N_c} \left(\frac{\mu^2}{m_b^2} \right)^\varepsilon \left\{ \frac{t_3(u)}{\varepsilon} + t_4(u) + \mathcal{O}(\varepsilon) \right\} F^{(0)} \Phi^{(0)} \quad (15)$$

and an additional μ -dependent contribution to the physical kernel from

$$F_E^{(0)} \text{Re } T_{1,E}^{(1)} \Phi_{\text{amp},E}^{(1)} \rightarrow \frac{C_F^2}{N_c} \left\{ 12L + t_{E,2}(u) + \mathcal{O}(\varepsilon) \right\} F^{(0)} \Phi^{(0)}. \quad (16)$$

Colour-suppressed tree amplitude

In this case we find an analogous set of operators,

$$\begin{aligned} \tilde{\mathcal{O}} &= [\gamma^\mu L] \tilde{\otimes} [\gamma_\mu L], \\ \tilde{\mathcal{O}}_E &= [\gamma^\mu \gamma^\nu \gamma^\rho L] \tilde{\otimes} [\gamma_\mu \gamma_\nu \gamma_\rho L] - 16 \tilde{\mathcal{O}}, \\ \tilde{\mathcal{O}}_{E'} &= [\gamma^\mu \gamma^\nu \gamma^\rho \gamma^\sigma \gamma^\tau L] \tilde{\otimes} [\gamma_\mu \gamma_\nu \gamma_\rho \gamma_\sigma \gamma_\tau L] - 20 \tilde{\mathcal{O}}_E - 256 \tilde{\mathcal{O}}, \end{aligned} \quad (17)$$

but the fields are now given in the wrong ordering $\bar{u}(y)[y, x]\Gamma_1 b(x)$ and $\bar{d}(x)\Gamma_2 u(x)$ (indicated by $\tilde{\otimes}$), which does not yield a form factor and a light-cone distribution amplitude. The latter follow from the factorized hadronic matrix element of the operator

$$\mathcal{O} = \bar{d}(x)\gamma^\mu L b(x) \otimes \bar{u}(y)[y, x]\gamma_\mu L u(x), \quad (18)$$

which is the Fierz-symmetric counterpart of $\tilde{\mathcal{O}}$. We therefore extend the right hand side of (10) to include four operators in this case: the physical operator \mathcal{O} , the evanescent operators $\tilde{\mathcal{O}}_E$ and $\tilde{\mathcal{O}}_{E'}$ and the Fierz-evanescent operator $\tilde{\mathcal{O}}_F \equiv \tilde{\mathcal{O}} - \mathcal{O}$.

The IR subtractions turn out to be particularly complicated in this case, due to the fact that the evanescent operator $\tilde{\mathcal{O}}_F$ already appears in the tree level calculation. As a consequence the naive split-up into non-factorizable diagrams, which contribute to the hard-scattering kernels, and factorizable diagrams, which give form factor and wave function corrections, is spoiled. In NLO we find that equations (30) and (31) of [5] should be replaced by⁸

$$\begin{aligned} \langle \hat{Q}_i \rangle_{\text{nf}}^{(1)} + Z_{ij}^{(1)} \langle \hat{Q}_j \rangle^{(0)} &= \hat{F}^{(0)} \cdot \hat{T}_i^{(1)} \otimes \hat{\Phi}^{(0)} + \hat{\Delta}_{F,i}^{(1)}, \\ \langle \hat{Q}_i \rangle_{\text{f}}^{(1)} + Z_\psi^{(1)} \langle \hat{Q}_i \rangle^{(0)} &= \hat{F}^{(1)} \cdot \hat{T}_i^{(0)} \otimes \hat{\Phi}^{(0)} + \hat{F}^{(0)} \cdot \hat{T}_i^{(0)} \otimes \hat{\Phi}^{(1)} - \hat{\Delta}_{F,i}^{(1)}, \end{aligned} \quad (19)$$

where $\hat{\Delta}_{F,i}^{(1)}$ contains the (non-vanishing) 1-loop counterterms of the form factor and wave function corrections for the Fierz-evanescent operator $\tilde{\mathcal{O}}_F$. In other words, the split-up in the above example of the colour-allowed tree amplitude followed from the fact that the corresponding counterterms vanish for the physical operator \mathcal{O} (i.e. $\Delta_i^{(k)} = 0$).

From the first equation in (19) we see that we can neglect the factorizable 1-loop diagrams in the computation of the NLO kernels. In order to account for the counterterm

⁸We introduce the "hat" notation to distinguish these quantities from those of the preceding section.

contribution $\hat{\Delta}_{F,i}^{(1)}$, we compute the UV-divergences of the 1-loop diagrams from Figure 5 and 6 of [5] with an insertion of the Fierz-evanescent operator $\tilde{\mathcal{O}}_F$. We find that the counterterms (ct) are given by

$$\begin{aligned}\hat{F}_F^{(1)} \hat{\Phi}_F^{(0)}|_{\text{ct}}(u) &= C_F \left\{ \hat{F}^{(0)} \hat{\Phi}^{(0)}(u) + \frac{1}{4\varepsilon} \hat{F}_E^{(0)} \hat{\Phi}_E^{(0)}(u) \right\}, \\ \hat{F}_F^{(0)} \hat{\Phi}_F^{(1)}|_{\text{ct}}(u) &= 2C_F \int_0^1 dw V_E(u, w) \left\{ \hat{F}^{(0)} \hat{\Phi}^{(0)}(w) + \frac{1}{4\varepsilon} \hat{F}_E^{(0)} \hat{\Phi}_E^{(0)}(w) \right\},\end{aligned}\quad (20)$$

with $V_E(u, w)$ from equation (45) of [5]. Convoluting these expressions with the LO kernels, $\hat{T}_{1,F}^{(0)} = C_F/N_c$ and $\hat{T}_{2,F}^{(0)} = 1/N_c$, yields the additional counterterm contributions

$$\hat{\Delta}_{F,1}^{(1)} = C_F \hat{\Delta}_{F,2}^{(1)} = \frac{2C_F^2}{N_c} \left\{ \hat{F}^{(0)} \hat{\Phi}^{(0)} + \frac{1}{4\varepsilon} \hat{F}_E^{(0)} \hat{\Phi}_E^{(0)} \right\}. \quad (21)$$

With this prescription the NLO kernels turn out to be free of IR-singularities. Evaluating the first equation of (19) to $\mathcal{O}(\varepsilon^2)$ gives (in terms of $T_1^{(1)}$ from (14)),

$$\begin{aligned}\hat{T}_1^{(1)}(u) + C_F &= -\frac{\hat{T}_2^{(1)}(u)}{2N_c} \\ &= -\frac{T_1^{(1)}(u)}{N_c} - \frac{C_F}{2N_c^2} \left(\frac{\mu^2}{m_b^2} \right)^\varepsilon \left\{ \left(\hat{t}_1(u) + 2L \right) \varepsilon + \left(\hat{t}_2(u) - L^2 \right) \varepsilon^2 + \mathcal{O}(\varepsilon^3) \right\}, \\ \hat{T}_{1,E}^{(1)}(u) &= -\frac{\hat{T}_{2,E}^{(1)}(u)}{2N_c} = \frac{C_F}{8N_c^2} \left(\frac{\mu^2}{m_b^2} \right)^\varepsilon \left\{ 2L + \hat{t}_{E,0}(u) + \left(\hat{t}_{E,1}(u) - L^2 \right) \varepsilon + \mathcal{O}(\varepsilon^2) \right\}, \\ \hat{T}_{1,F}^{(1)}(u) &= -\frac{\hat{T}_{2,F}^{(1)}(u)}{2N_c} = -\frac{T_1^{(1)}(u)}{N_c} - \frac{C_F}{2N_c^2} \left(\frac{\mu^2}{m_b^2} \right)^\varepsilon \left\{ 2 + \hat{t}_1(u) \varepsilon + \mathcal{O}(\varepsilon^2) \right\}.\end{aligned}\quad (22)$$

We next compute form factor and wave function corrections to \mathcal{O} , $\tilde{\mathcal{O}}_E$ and $\tilde{\mathcal{O}}_F$. Proceeding along the lines outlined in Section 4.3 of [5], we obtain⁹

$$\begin{aligned}\hat{F}_{\text{amp,E}}^{(1)} \hat{\Phi}_E^{(0)} &= C_F \left[24 - \left(\frac{e^{\gamma_E} \mu^2}{m_b^2} \right)^\varepsilon \Gamma(\varepsilon) \frac{24\varepsilon(1+\varepsilon)}{(1-\varepsilon)^2} \right] \hat{F}^{(0)} \hat{\Phi}^{(0)} \\ &\quad - C_F \left[\frac{3}{\varepsilon} + \left(\frac{e^{\gamma_E} \mu^2}{m_b^2} \right)^\varepsilon \Gamma(\varepsilon) \frac{1-6\varepsilon+16\varepsilon^2-14\varepsilon^3}{\varepsilon(1-2\varepsilon)(1-\varepsilon)^2} \right] \hat{F}_E^{(0)} \hat{\Phi}_E^{(0)} \\ &\quad + C_F \left[\frac{1}{4\varepsilon} - \left(\frac{e^{\gamma_E} \mu^2}{m_b^2} \right)^\varepsilon \frac{\Gamma(\varepsilon)}{4(1-\varepsilon)^2} \right] \hat{F}_{E'}^{(0)} \hat{\Phi}_{E'}^{(0)} \\ &\quad - C_F \left(\frac{e^{\gamma_E} \mu^2}{m_b^2} \right)^\varepsilon \Gamma(\varepsilon) \frac{24\varepsilon(1+\varepsilon)}{(1-\varepsilon)^2} \hat{F}_F^{(0)} \hat{\Phi}_F^{(0)}, \\ \hat{F}_{\text{amp,F}}^{(1)} \hat{\Phi}_F^{(0)} &= C_F \left[1 - \left(\frac{e^{\gamma_E} \mu^2}{m_b^2} \right)^\varepsilon \Gamma(\varepsilon) \left(\frac{1-3\varepsilon+6\varepsilon^2-6\varepsilon^3}{\varepsilon(1-2\varepsilon)(1-\varepsilon)^2} - \frac{1-\varepsilon+2\varepsilon^2}{\varepsilon(1-2\varepsilon)} \right) \right] \hat{F}^{(0)} \hat{\Phi}^{(0)}\end{aligned}$$

⁹The corrections to the physical operator \mathcal{O} can be found in [5].

$$\begin{aligned}
& + C_F \left[\frac{1}{4\varepsilon} - \left(\frac{e^{\gamma_E} \mu^2}{m_b^2} \right)^\varepsilon \frac{\Gamma(\varepsilon)}{4(1-\varepsilon)^2} \right] \hat{F}_E^{(0)} \hat{\Phi}_E^{(0)} \\
& - C_F \left(\frac{e^{\gamma_E} \mu^2}{m_b^2} \right)^\varepsilon \Gamma(\varepsilon) \frac{1-3\varepsilon+6\varepsilon^2-6\varepsilon^3}{\varepsilon(1-2\varepsilon)(1-\varepsilon)^2} \hat{F}_F^{(0)} \hat{\Phi}_F^{(0)}
\end{aligned} \tag{23}$$

and for the wave function corrections

$$\begin{aligned}
\hat{F}_E^{(0)} \hat{\Phi}_{\text{amp},E}^{(1)} &= 48C_F \left[V_E \otimes \hat{F}^{(0)} \hat{\Phi}^{(0)} \right] - \frac{2C_F}{\varepsilon} \left[(V + 3V_E) \otimes \hat{F}_E^{(0)} \hat{\Phi}_E^{(0)} \right] \\
&+ \frac{C_F}{2\varepsilon} \left[V_E \otimes \hat{F}_{E'}^{(0)} \hat{\Phi}_{E'}^{(0)} \right], \\
\hat{F}_F^{(0)} \hat{\Phi}_{\text{amp},F}^{(1)} &= 2C_F \left[V_E \otimes \hat{F}^{(0)} \hat{\Phi}^{(0)} \right] + \frac{C_F}{2\varepsilon} \left[V_E \otimes \hat{F}_E^{(0)} \hat{\Phi}_E^{(0)} \right] - \frac{2C_F}{\varepsilon} \left[V \otimes \hat{F}_F^{(0)} \hat{\Phi}_F^{(0)} \right],
\end{aligned} \tag{24}$$

where \otimes represents a convolution and V is the Efremov-Radyushkin-Brodsky-Lepage (ERBL) kernel [18] (given explicitly in equation (43) of [5]). We finally compute the convolutions of the NLO kernels with the wave function corrections. For the physical operator \mathcal{O} we get

$$\begin{aligned}
\hat{F}^{(0)} \hat{T}_1^{(1)} \hat{\Phi}_{\text{amp}}^{(1)} &= -\frac{1}{2N_c} \hat{F}^{(0)} \hat{T}_2^{(1)} \hat{\Phi}_{\text{amp}}^{(1)} \\
&= -\frac{1}{N_c} F^{(0)} T_1^{(1)} \Phi_{\text{amp}}^{(1)} + \frac{C_F^2}{2N_c^2} \left\{ \hat{t}_3(u) + \mathcal{O}(\varepsilon) \right\} \hat{F}^{(0)} \hat{\Phi}^{(0)},
\end{aligned} \tag{25}$$

while the evanescent operators give again μ -dependent corrections to the physical kernels

$$\begin{aligned}
\hat{F}_E^{(0)} \hat{T}_{1,E}^{(1)} \hat{\Phi}_{\text{amp},E}^{(1)} &= -\frac{1}{2N_c} \hat{F}_E^{(0)} \hat{T}_{2,E}^{(1)} \hat{\Phi}_{\text{amp},E}^{(1)} \rightarrow \frac{C_F^2}{N_c^2} \left\{ 6L + \hat{t}_{E,2}(u) + \mathcal{O}(\varepsilon) \right\} \hat{F}^{(0)} \hat{\Phi}^{(0)}, \\
\hat{F}_F^{(0)} \hat{T}_{1,F}^{(1)} \hat{\Phi}_{\text{amp},F}^{(1)} &= -\frac{1}{2N_c} \hat{F}_F^{(0)} \hat{T}_{2,F}^{(1)} \hat{\Phi}_{\text{amp},F}^{(1)} \rightarrow \frac{C_F^2}{2N_c^2} \left\{ 6L + \hat{t}_{F,0}(u) + \mathcal{O}(\varepsilon) \right\} \hat{F}^{(0)} \hat{\Phi}^{(0)}.
\end{aligned} \tag{26}$$

According to (12) we now have assembled all pieces to perform the IR subtractions in NNLO. However, as we have seen above in the calculation of the NLO kernels, the naive split-up into factorizable and non-factorizable contributions is spoiled for the colour-suppressed amplitude. In analogy to (19) we therefore have to account for an additional contribution $\hat{\Delta}_{F,i}^{(2)}$ on the right hand side of (12), which represents the 2-loop counterterms of the form factor and wave function corrections for the Fierz-evanescent operator $\tilde{\mathcal{O}}_F$.

The calculation of this counterterm contribution requires a rather complicated 2-loop calculation on its own. We refer to Appendix B for the details of this calculation and quote the contribution to the physical kernel only,

$$\begin{aligned}
\hat{\Delta}_{F,1}^{(2)} = C_F \hat{\Delta}_{F,2}^{(2)} &\rightarrow -\frac{2C_F^2}{N_c} \left\{ \frac{C_F}{\varepsilon^2} + \left[(1+L)C_F + \frac{11}{6}C_A - \frac{1}{3}n_f \right] \frac{1}{\varepsilon} \right. \\
&\left. + \left(28 + \frac{\pi^2}{12} + 7L + \frac{1}{2}L^2 \right) C_F - \frac{149}{36}C_A - \frac{5}{18}n_f + \mathcal{O}(\varepsilon) \right\} \hat{F}^{(0)} \hat{\Phi}^{(0)}.
\end{aligned} \tag{27}$$

3 Vertex corrections in NNLO

As we have seen in the last section, the NNLO calculation of the hard-scattering kernels requires a rather complex subtraction procedure of UV- and IR-divergences. The fact that the kernels turn out to be free of any singularities represents both a non-trivial confirmation of the factorization framework and a stringent cross-check of our calculation.

3.1 Hard-scattering kernels

In terms of the Wilson coefficients C_i of the physical operators Q_i from the operator basis (3), the topological tree amplitudes take to NNLO the form

$$\begin{aligned}
\alpha_1(M_1 M_2) &= C_2 + \frac{\alpha_s}{4\pi} \frac{C_F}{2N_c} \left\{ C_1 V^{(1)} + \frac{\alpha_s}{4\pi} \left[C_1 V_1^{(2)} + C_2 V_2^{(2)} \right] + \mathcal{O}(\alpha_s^2) \right\} + \dots \\
\alpha_2(M_1 M_2) &= \frac{C_F}{N_c} C_1 + \frac{C_2}{N_c} + \frac{\alpha_s}{4\pi} \frac{C_F}{2N_c} \left\{ \left(2C_2 - \frac{C_1}{N_c} \right) V^{(1)} - 2C_A C_1 \right. \\
&\quad + \frac{\alpha_s}{4\pi} \left[\left(2C_2 - \frac{C_1}{N_c} \right) V_1^{(2)} + \left(\frac{C_F}{N_c} C_1 + \frac{C_2}{N_c} \right) V_2^{(2)} + 2C_A C_2 V^{(1)} \right. \\
&\quad \left. \left. + \left(8C_F - \frac{113}{18} C_A - \frac{5}{9} n_f \right) C_A C_1 \right] + \mathcal{O}(\alpha_s^2) \right\} + \dots \quad (28)
\end{aligned}$$

where the ellipsis refer to the terms from spectator scattering which we disregard in the following. In this notation the α_s corrections have been expressed in terms of the convolution

$$V^{(1)} = \int_0^1 du \left(-6L + g_2(u) + i\pi g_1(u) \right) \phi_{M_2}(u), \quad (29)$$

where $L = \ln \mu^2/m_b^2$ and (recall that $\bar{u} = 1 - u$)

$$\begin{aligned}
g_1(u) &= -3 - 2 \ln u + 2 \ln \bar{u}, \\
g_2(u) &= -22 + \frac{3(1-2u)}{\bar{u}} \ln u + \left[2\text{Li}_2(u) - \ln^2 u - \frac{1-3u}{\bar{u}} \ln u - (u \rightarrow \bar{u}) \right]. \quad (30)
\end{aligned}$$

If we transform these expressions into the Fierz-symmetric operator basis that has been used in many previous QCD factorization analyses, we reproduce the NLO result from [1]. In NNLO we find the convolutions

$$\begin{aligned}
V_1^{(2)} &= \int_0^1 du \left\{ \left(36C_F - 29C_A + 2n_f \right) L^2 \right. \\
&\quad + \left\{ \left(\frac{29}{3} C_A - \frac{2}{3} n_f \right) g_2(u) - \frac{91}{6} C_A - \frac{10}{3} n_f + C_F h_6(u) \right. \\
&\quad \left. \left. + i\pi \left[\left(\frac{29}{3} C_A - \frac{2}{3} n_f \right) g_1(u) + C_F h_1(u) \right] \right\} L \right\}
\end{aligned}$$

$$\begin{aligned}
& + C_F h_7(u) + C_A h_8(u) + (n_f - 2) h_9(u; 0) + h_9(u; z) + h_9(u; 1) \\
& + i\pi \left[C_F h_2(u) + C_A h_3(u) + (n_f - 2) h_4(u; 0) + h_4(u; z) + h_4(u; 1) \right] \Big\} \phi_{M_2}(u), \\
V_2^{(2)} = & \int_0^1 du \left\{ 18L^2 + \left(21 - 6g_2(u) - 6i\pi g_1(u) \right) L + h_5(u) + i\pi h_0(u) \right\} \phi_{M_2}(u), \quad (31)
\end{aligned}$$

where $n_f = 5$ represents the number of active quark flavours and $z = m_c/m_b$. The explicit expressions for the NNLO kernels h_{0-4} , which specify the imaginary parts of the topological tree amplitudes, can be found in [5]. As a new result we obtained the real parts of the topological tree amplitudes to NNLO, which have been given in terms of a new set of kernels h_{5-9} that are listed in Appendix C.

Partial structures of our NNLO result can be cross-checked. First, we verified that the scale dependence between the Wilson coefficients, the coupling constant, the hard-scattering kernels and the light-cone distribution amplitude cancels in the tree amplitudes $\alpha_i(M_1 M_2)$ to $\mathcal{O}(\alpha_s^2)$ as it should¹⁰. Second, we compared the terms proportional to n_f with the analysis of the large β_0 -limit in [19] and found agreement. Finally, we reproduced the imaginary part of the colour-suppressed amplitude from our earlier analysis in [5], which was derived on the basis of Fierz-symmetry arguments.

3.2 Convolutions in Gegenbauer expansion

We expand the light-cone distribution amplitude of the emitted meson M_2 into the eigenfunctions of the 1-loop evolution kernel,

$$\phi_{M_2}(u) = 6u\bar{u} \left[1 + \sum_{n=1}^{\infty} a_n^{M_2} C_n^{(3/2)}(2u-1) \right], \quad (32)$$

where $a_n^{M_2}$ and $C_n^{(3/2)}$ are the Gegenbauer moments and polynomials, respectively. It is convenient to truncate this expansion at $n = 2$, which allows us to perform the convolution integrals in our final expression (31) explicitly. The convolution with the NLO kernel results in¹¹,

$$\int_0^1 du g_2(u) \phi_{M_2}(u) = -\frac{45}{2} + \frac{11}{2} a_1^{M_2} - \frac{21}{20} a_2^{M_2}, \quad (33)$$

whereas the convolutions with the NNLO kernels become

$$\begin{aligned}
\int_0^1 du h_5(u) \phi_{M_2}(u) = & \frac{5347}{60} - \frac{14833}{5} \zeta_3 + 3744 \zeta_5 \\
& + \left(\frac{12487}{12} - 936 \zeta_3 + 72 \ln 2 \right) \pi^2 + \frac{239\pi^4}{90}
\end{aligned}$$

¹⁰We emphasize that this cancellation would have been incomplete, if μ -dependent contributions from the mixing of evanescent operators as e.g. in (16) or (26) had been missed.

¹¹We refer to [5] for the convolutions with the kernels g_1 and h_{0-4} .

$$\begin{aligned}
& + \left\{ \frac{4568}{15} + \frac{77157}{5} \zeta_3 - 19008 \zeta_5 \right. \\
& \quad \left. - \left(\frac{21807}{4} - 4752 \zeta_3 + 24 \ln 2 \right) \pi^2 - \frac{181\pi^4}{10} \right\} a_1^{M_2} \\
& + \left\{ \frac{32369221}{12600} - \frac{2236872}{35} \zeta_3 + 74304 \zeta_5 \right. \\
& \quad \left. + \left(\frac{204218}{9} - 18576 \zeta_3 - 2064 \ln 2 \right) \pi^2 + \frac{797\pi^4}{10} \right\} a_2^{M_2}, \\
\int_0^1 du h_6(u) \phi_{M_2}(u) &= 348 - \frac{154}{3} a_1^{M_2} + \frac{329}{40} a_2^{M_2}, \\
\int_0^1 du h_7(u) \phi_{M_2}(u) &= \frac{12809}{60} - \frac{26606}{5} \zeta_3 + 6564 \zeta_5 \\
& \quad + \left(\frac{12811}{6} - 1764 \zeta_3 - 48 \ln 2 \right) \pi^2 + \frac{134\pi^4}{45} \\
& + \left\{ \frac{50387}{180} + \frac{132294}{5} \zeta_3 - 32472 \zeta_5 \right. \\
& \quad \left. - \left(\frac{66425}{6} - 8856 \zeta_3 - 1296 \ln 2 \right) \pi^2 - \frac{176\pi^4}{5} \right\} a_1^{M_2} \\
& + \left\{ \frac{75807647}{12600} - \frac{3960924}{35} \zeta_3 + 129204 \zeta_5 \right. \\
& \quad \left. + \left(\frac{2074841}{45} - 34884 \zeta_3 - 8672 \ln 2 \right) \pi^2 + \frac{727\pi^4}{5} \right\} a_2^{M_2}, \\
\int_0^1 du h_8(u) \phi_{M_2}(u) &= -\frac{74611}{180} + \frac{618}{5} \zeta_3 - 186 \zeta_5 \\
& \quad - \left(\frac{815}{6} - 108 \zeta_3 - 36 \ln 2 \right) \pi^2 - \frac{169\pi^4}{120} \\
& + \left\{ \frac{355693}{360} + \frac{10818}{5} \zeta_3 - 2556 \zeta_5 \right. \\
& \quad \left. - \left(\frac{1081}{12} - 270 \zeta_3 + 684 \ln 2 \right) \pi^2 + \frac{151\pi^4}{8} \right\} a_1^{M_2} \\
& + \left\{ -\frac{148920211}{25200} + \frac{128283}{35} \zeta_3 - 666 \zeta_5 \right. \\
& \quad \left. - \left(\frac{66545}{18} - 1458 \zeta_3 - 4120 \ln 2 \right) \pi^2 - \frac{1403\pi^4}{20} \right\} a_2^{M_2}.
\end{aligned} \tag{34}$$

We finally perform the convolution with the hard-scattering kernel $h_9(u; z_f)$, which stems from the diagrams with a closed fermion loop. As this contribution depends on the mass $m_f = z_f m_b$ of the internal quark, we parameterize the convolution as

$$\int_0^1 du h_9(u; z_f) \phi_{M_2}(u) = H_{9,0}(z_f) + H_{9,1}(z_f) a_1^{M_2} + H_{9,2}(z_f) a_2^{M_2}. \quad (35)$$

For massless quarks we may perform the convolution integral analytically,

$$\int_0^1 du h_9(u; 0) \phi_{M_2}(u) = \frac{493}{18} - \frac{2\pi^2}{3} - \left(\frac{40}{3} + 2\pi^2\right) a_1^{M_2} + \left(\frac{8059}{600} - \pi^2\right) a_2^{M_2}, \quad (36)$$

whereas we obtain numerical results for massive internal quarks. In Table 1 we summarize the contributions from closed fermion loops for massless quarks ($z_q = 0$), for a b -quark ($z_b = 1$) and for a charm quark ($z_c \in [0.25, 0.35]$).

We illustrate the relative importance of the individual contributions setting $\mu = m_b$ and $z_c = m_c/m_b = 0.3$, which yields (with $C_F = 4/3$, $C_A = 3$, $n_f = 5$)

$$\begin{aligned} V^{(1)} &= (-22.500 - 9.425 i) + (5.500 - 9.425 i) a_1^{M_2} + (-1.050) a_2^{M_2}, \\ V_1^{(2)} &= (-178.38 - 349.44 i) + (660.59 - 119.36 i) a_1^{M_2} + (-85.40 - 62.63 i) a_2^{M_2}, \\ V_2^{(2)} &= (322.19 + 320.94 i) + (-212.97 + 154.41 i) a_1^{M_2} + (3.81 - 34.06 i) a_2^{M_2}. \end{aligned} \quad (37)$$

We find relatively large coefficients for the NNLO terms and expect only a minor impact of the higher Gegenbauer moments in the symmetric case with $a_1^{M_2} = 0$.

We conclude with a remark concerning the large β_0 -limit that has been considered in [19]. In this approximation we get

$$V_1^{(2)}|_{\beta_0} \simeq (-239.31 - 264.94 i) + (380.33 - 252.90 i) a_1^{M_2} + (-40.96 - 21.68 i) a_2^{M_2}, \quad (38)$$

whereas the contribution from $V_2^{(2)}$ is completely missed. As a consequence the NNLO contribution to α_1 is substantially underestimated in this approximation, whereas the one to α_2 deviates from the full NNLO result between $\sim 15\%$ for the imaginary part and $\sim 40\%$ for the real part. This illustrates the importance of performing exact 2-loop calculations.

z_f	0	0.25	0.275	0.3	0.325	0.35	1
$H_{9,0}$	20.81	17.12	16.43	15.72	14.99	14.26	-3.62
$H_{9,1}$	-33.07	-13.28	-12.37	-11.54	-10.77	-10.07	-0.68
$H_{9,2}$	3.56	2.08	1.94	1.81	1.68	1.57	0.01

Table 1: *Fermionic contribution in the notation of (35). The first column refers to massless quarks, the last column to the b -quark and the other columns to the charm quark for different physical values of $z_c = m_c/m_b$.*

4 Numerical analysis

We conclude with a brief analysis of the numerical impact of the considered NNLO corrections. As a phenomenological analysis of hadronic B decays is beyond the scope of the present paper, we focus on the perturbative structure of the topological tree amplitudes and discuss their remnant uncertainties. In particular, we now combine our results with the NNLO corrections from 1-loop spectator scattering that have been worked out in [3].

4.1 Implementation of spectator scattering

In contrast to the vertex corrections considered in this work, the spectator scattering term is sensitive to two perturbative scales: the hard scale $\mu_h \sim m_b$ and a dynamically generated intermediate (hard-collinear) scale $\mu_{hc} \sim (\Lambda_{\text{QCD}} m_b)^{1/2}$. The hard scattering kernels from spectator scattering therefore factorize further into coefficient functions H_i^{II} , encoding the hard effects, and a universal hard-collinear jet-function $J_{||}$. Renormalization group techniques can be used to resum parametrically large logarithms of the form $\ln m_b/\Lambda_{\text{QCD}}$ in terms of an evolution kernel $\mathcal{U}_{||}$. Following the first paper of [3], we implement the spectator scattering contribution to the topological tree amplitudes as¹²

$$\begin{aligned} & C_i(\mu) T_i^{II}(\mu) \otimes [\hat{f}_B \phi_B](\mu) \otimes \phi_{M_1}(\mu) \otimes \phi_{M_2}(\mu) \\ & \rightarrow C_i(\mu_h) H_i^{II}(\mu_h) \otimes \mathcal{U}_{||}(\mu_h, \mu_{hc}) \otimes J_{||}(\mu_{hc}) \otimes [\hat{f}_B \phi_B](\mu_{hc}) \otimes \phi_{M_1}(\mu_{hc}) \otimes \phi_{M_2}(\mu_h). \end{aligned} \quad (39)$$

Since the spectator scattering starts at $\mathcal{O}(\alpha_s)$, the resummation is required here in the next-to-leading-logarithmic (NLL) approximation. Unfortunately, a complete NLL resummation is not possible since the evolution kernel $\mathcal{U}_{||}$ is known in the leading-logarithmic (LL) approximation only [20].

We therefore proceed along the lines of our earlier analysis [5], where we worked in the LL approximation which is consistent for the imaginary parts that are of $\mathcal{O}(\alpha_s^2)$. According to this, we implement the LL evolution of the HQET decay constant and the Gegenbauer moments to evolve the hadronic parameters from their input scales to the ones required in (39). The B meson distribution amplitude is modeled according to [21], which implies $\lambda_B(1\text{GeV}) = (0.48 \pm 0.12)\text{GeV}$ and, for the first two logarithmic moments, $\sigma_1(1\text{GeV}) = 1.6 \pm 0.2$ and $\sigma_2(1\text{GeV}) = 3.3 \pm 0.8$. The 1-loop matching corrections to the hard functions H_i^{II} [3] and the jet function $J_{||}$ [20, 22] are implemented neglecting crossed terms of $\mathcal{O}(\alpha_s^3)$. We finally adopt the BBNS model from [1] to estimate the size of power corrections to the factorization formula.

In the spectator scattering term we compute the Wilson coefficients from the effective weak Hamiltonian in the NLL approximation with 2-loop running coupling constant. Quantities referring to the hard scale are evaluated in a theory with $n_f = 5$ flavours and those referring to the hard-collinear scale with $n_f = 4$.

¹²One should keep in mind that the Wilson coefficients in the spectator scattering term refer to a different operator basis than the one used in the current work (namely the Fierz-symmetric *traditional basis* that we denoted by a tilde in [5]).

4.2 Tree amplitudes in NNLO

We finally evaluate the topological tree amplitudes for the $B \rightarrow \pi\pi$ channels using the input parameters from our earlier analysis [5] and computing the Wilson coefficients in the vertex corrections in the next-to-next-to-leading-logarithmic (NNLL) approximation [8, 23] with 3-loop running coupling constant [24] and $\Lambda_{\overline{\text{MS}}}^{(5)} = 205$ MeV. Under these specifications the NNLO prediction of the topological tree amplitudes becomes¹³

$$\begin{aligned}
\alpha_1(\pi\pi) &= 1.008|_{V^{(0)}} + [0.022 + 0.009i]_{V^{(1)}} + [0.024 + 0.026i]_{V^{(2)}} \\
&\quad - 0.012|_{S^{(1)}} - [0.014 + 0.011i]_{S^{(2)}} - 0.007|_P \\
&= 1.019^{+0.017}_{-0.021} + (0.025^{+0.019}_{-0.015})i, \\
\alpha_2(\pi\pi) &= 0.224|_{V^{(0)}} - [0.174 + 0.075i]_{V^{(1)}} - [0.030 + 0.048i]_{V^{(2)}} \\
&\quad + 0.075|_{S^{(1)}} + [0.032 + 0.019i]_{S^{(2)}} + 0.045|_P \\
&= 0.173^{+0.088}_{-0.073} - (0.103^{+0.051}_{-0.054})i.
\end{aligned} \tag{40}$$

Here we disentangled the contributions of the various terms in the factorization formula, namely the tree level result $V^{(0)}$ ("naive factorization"), NLO (1-loop) vertex corrections $V^{(1)}$, NNLO (2-loop) vertex corrections $V^{(2)}$, NLO (tree level) spectator scattering $S^{(1)}$, NNLO (1-loop) spectator scattering $S^{(2)}$ and the modelled power corrections P .

The new contributions from this work consist in the real parts of the terms denoted by $V^{(2)}$. For the colour-allowed amplitude $\alpha_1(\pi\pi)$, this correction is slightly larger than the α_s terms due to an numerical enhancement from the Wilson coefficients in the effective Hamiltonian¹⁴. On the other hand, the colour-suppressed amplitude $\alpha_2(\pi\pi)$ receives a

¹³The numbers for the imaginary parts differ slightly from those of [5], since we now evaluate the Wilson coefficients throughout in the NNLL approximation.

¹⁴We remark that a similar enhancement is unlikely to exist at even higher order of the perturbative expansion, since the NNLO expressions already reveal the full complexity.

	μ_h	μ_{hc}	f_B	$F_+^{B\pi}$	λ_B	a_2^π	X_H
$\text{Re}(\alpha_1)$	+0.008 −0.011	+0.006 −0.007	+0.003 −0.003	+0.006 −0.008	+0.006 −0.009	+0.007 −0.008	+0.007 −0.007
$\text{Im}(\alpha_1)$	+0.017 −0.011	+0.002 −0.003	+0.001 −0.001	+0.002 −0.003	+0.002 −0.003	+0.004 −0.004	+0.007 −0.007
$\text{Re}(\alpha_2)$	+0.016 −0.008	+0.026 −0.023	+0.014 −0.014	+0.038 −0.025	+0.039 −0.026	+0.038 −0.033	+0.045 −0.045
$\text{Im}(\alpha_2)$	+0.019 −0.028	+0.005 −0.004	+0.002 −0.002	+0.005 −0.003	+0.005 −0.003	+0.007 −0.006	+0.045 −0.045

Table 2: *Dominant uncertainties of our final predictions for the colour-allowed tree amplitudes $\alpha_1(\pi\pi)$ and the colour-suppressed tree amplitude $\alpha_2(\pi\pi)$ from scale variations, hadronic input parameters and modelled power corrections.*

moderate correction. In particular, we do not find an enhancement of the phenomenologically interesting ratio $|\alpha_2/\alpha_1|$ from the perturbative calculation.

In Table 2 we list the uncertainties of our NNLO predictions stemming from scale variations, hadronic input parameters and the modelled power corrections. The values of the first two columns follow from varying the perturbative scales independently in the ranges $\mu_h = 4.8^{+4.8}_{-2.4}$ GeV and $\mu_{hc} = 1.5^{+0.9}_{-0.5}$ GeV. As the dependence on the hard scale tends to cancel between vertex corrections and spectator scattering, we vary both contributions independently and take the larger interval (from the vertex corrections) as our estimate for higher order perturbative corrections. The scale dependence of the vertex corrections is also illustrated in Figure 2, where we read off that it gets substantially reduced for the real parts at NNLO, whereas the reduction is less pronounced for the imaginary parts.

For our final error estimate in (40) we added the individual uncertainties from Table 2 in quadrature. Whereas the colour-allowed amplitude $\alpha_1(\pi\pi)$ can be computed precisely in the factorization framework, the situation is less fortunate for the colour-suppressed amplitude $\alpha_2(\pi\pi)$. Due to large cancellations between the vertex corrections, the colour-suppressed amplitude becomes particularly sensitive to the spectator scattering contribution and is therefore subject to rather large uncertainties related mainly to our restricted knowledge of the hadronic input parameters.

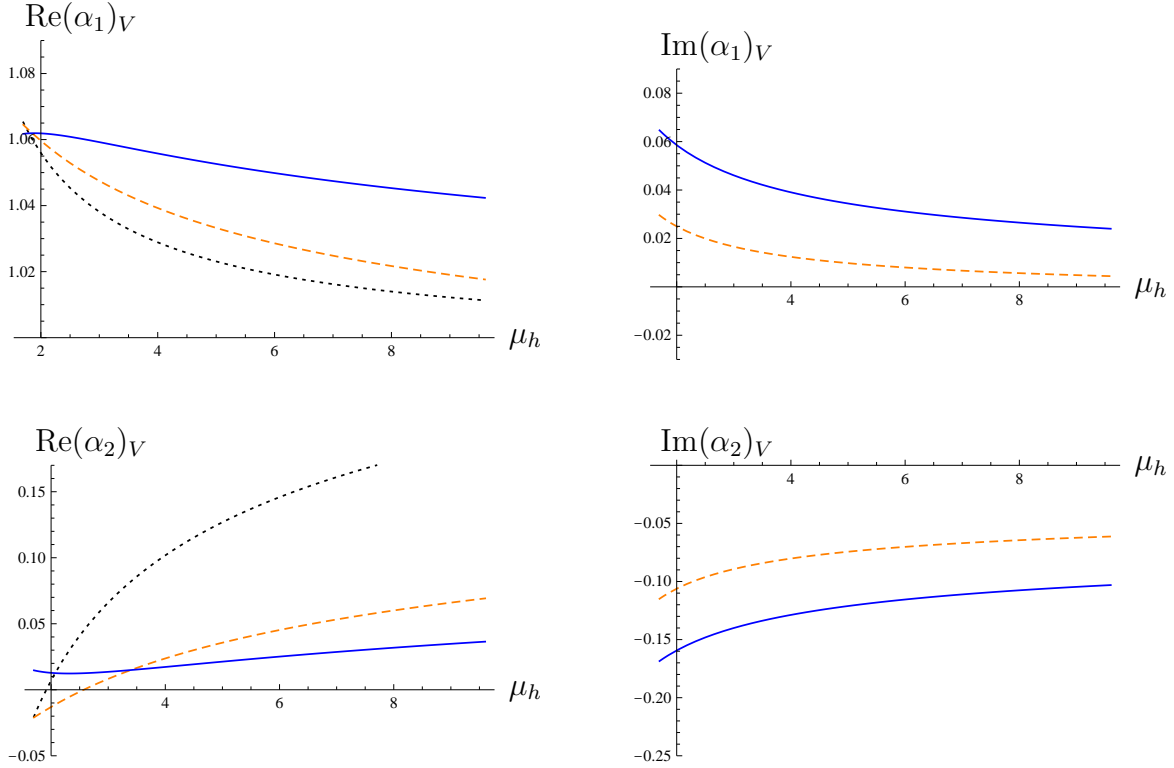


Figure 2: Dependence of the tree amplitudes $\alpha_i(\pi\pi)$ as a function of the hard scale μ_h (vertex corrections only). The dotted (black) lines refer to LO, the dashed (orange/light gray) lines to NLO and the solid (blue/dark gray) lines to NNLO.

5 Conclusion

We computed the real parts of the 2-loop vertex corrections for charmless hadronic B meson decays, completing the NNLO calculation of the topological tree amplitudes in the QCD factorization framework. We in particular showed how to compute the colour-suppressed tree amplitude without making use of Fierz-symmetry arguments and found that the hard-scattering kernels are free of IR-singularities and the resulting convolutions with the light-cone distribution amplitude of the emitted light meson are finite, which demonstrates factorization at the 2-loop order.

The numerical impact of the considered corrections was found to be moderate, although they can be of similar size as the NLO corrections. The scale dependence of the real parts of the topological tree amplitudes is significantly reduced at NNLO, which allows for a precise determination of the colour-allowed amplitude α_1 . In contrast to this, it remains difficult to compute the colour-suppressed amplitude α_2 in the factorization framework, since it is subject to substantial uncertainties from hadronic input parameters and potential $1/m_b$ corrections. In particular, we do not find an enhancement of the phenomenologically important ratio $|\alpha_2/\alpha_1|$ from the perturbative calculation.

Acknowledgements

We are grateful to Gerhard Buchalla for interesting discussions and helpful comments on the manuscript. This work was supported by the DFG Sonderforschungsbereich/Transregio 9.

A Auxiliary coefficient functions

In the calculation of the colour-allowed tree amplitude, the NLO kernels have been given in (14) in terms of the coefficient functions

$$\begin{aligned}
t_0(u) &= 4\text{Li}_2(u) - \ln^2 u + 2 \ln u \ln \bar{u} + \ln^2 \bar{u} + (2 - 3u) \left(\frac{\ln u}{\bar{u}} - \frac{\ln \bar{u}}{u} \right) - \frac{\pi^2}{3} - 22, \\
t_1(u) &= -2\text{Li}_3(u) - 2\text{S}_{1,2}(u) - 2 \ln \bar{u} \text{Li}_2(u) + \ln^3 u - 2 \ln^2 u \ln \bar{u} + \ln u \ln^2 \bar{u} - \ln^3 \bar{u} \\
&\quad + \frac{2 - 3u^2}{u\bar{u}} \text{Li}_2(u) - \frac{2 - 3u}{\bar{u}} \left(\ln^2 u - \ln u \ln \bar{u} \right) + \frac{6 - 11u + 2\bar{u}\pi^2}{\bar{u}} \ln u \\
&\quad + \frac{4 - 3u}{2u} \ln^2 \bar{u} - \frac{18 - 33u + 5u\pi^2}{3u} \ln \bar{u} + \frac{(7 - 6u)\pi^2}{6\bar{u}} + 2\zeta_3 - 52, \\
t_2(u) &= 10\text{Li}_4(u) - 8\text{S}_{2,2}(u) + 10\text{S}_{1,3}(u) - 8 \ln \bar{u} \text{Li}_3(u) + 10 \ln \bar{u} \text{S}_{1,2}(u) - \frac{7}{12} \ln^4 u \\
&\quad + 5 \ln^2 \bar{u} \text{Li}_2(u) + \frac{4}{3} \ln^3 u \ln \bar{u} - \ln^2 u \ln^2 \bar{u} + \frac{1}{3} \ln u \ln^3 \bar{u} + \frac{7}{12} \ln^4 \bar{u} \\
&\quad + \frac{2 - 6u + 6u^2}{u\bar{u}} \text{Li}_3(u) - \frac{4 - 6u + 3u^2}{u\bar{u}} \left(\text{S}_{1,2}(u) + \ln \bar{u} \text{Li}_2(u) \right) - \frac{8 - 3u}{6u} \ln^3 \bar{u}
\end{aligned}$$

$$\begin{aligned}
& + \frac{2-3u}{6\bar{u}} \left(4\ln^3 u - 6\ln^2 u \ln \bar{u} + 3\ln u \ln^2 \bar{u} \right) - \frac{60(1-2u) + 17\bar{u}\pi^2}{12\bar{u}} \ln^2 u \\
& + \frac{3(6-4u-7u^2) + u\bar{u}\pi^2}{3u\bar{u}} \text{Li}_2(u) + \frac{24-54u+5\bar{u}\pi^2}{6\bar{u}} \ln u \ln \bar{u} + \frac{(29-24u)\pi^2}{6\bar{u}} \\
& + \frac{6(12-13u) + 7u\pi^2}{12u} \ln^2 \bar{u} + \frac{24(7-13u) + (10-15u)\pi^2}{12\bar{u}} \ln u - \frac{23\pi^4}{180} \\
& - \frac{24\bar{u}(7-13u) + (2+23u-27u^2)\pi^2 + 24u\bar{u}\zeta_3}{12u\bar{u}} \ln \bar{u} + \frac{10-11u}{\bar{u}} \zeta_3 - 112, \\
t_{E,0}(u) &= -\frac{1-2u}{2} \left(\frac{\ln u}{\bar{u}} - \frac{\ln \bar{u}}{u} \right) + \frac{16}{3}, \\
t_{E,1}(u) &= -\frac{1-2u}{2u\bar{u}} \text{Li}_2(u) + \frac{1-3u}{4\bar{u}} \ln^2 u + \frac{u}{2\bar{u}} \ln u \ln \bar{u} - \frac{2-3u}{4u} \ln^2 \bar{u} \\
& - \frac{4(1-2u)}{3} \left(\frac{\ln u}{\bar{u}} - \frac{\ln \bar{u}}{u} \right) - \frac{(6-5u)\pi^2}{12\bar{u}} + 12
\end{aligned} \tag{41}$$

and the convolutions of the NLO kernels with the wave function corrections, cf. (15) and (16), involve

$$\begin{aligned}
t_3(u) &= 4\text{Li}_3(u) + 4\text{S}_{1,2}(u) - 4\ln u \text{Li}_2(u) + \frac{2}{3} \ln^3 u - 2\ln^2 u \ln \bar{u} - \frac{2}{3} \ln^3 \bar{u} - \frac{\text{Li}_2(u)}{u\bar{u}} \\
& - \frac{1-3u}{2u\bar{u}} \left(u \ln^2 u + 2\bar{u} \ln u \ln \bar{u} - \bar{u} \ln^2 \bar{u} \right) - \frac{3}{2u} \ln \bar{u} + \frac{(4-3u)\pi^2}{6\bar{u}} - \frac{15}{2} - 4\zeta_3, \\
t_4(u) &= 12\text{Li}_4(u) - 20\text{S}_{2,2}(u) + 12\text{S}_{1,3}(u) - 8 \left(\ln u + \ln \bar{u} \right) \text{Li}_3(u) + 12 \ln u \text{S}_{1,2}(u) \\
& + 4 \ln \bar{u} \text{S}_{1,2}(u) + \left(4\ln^2 u + 4\ln u \ln \bar{u} + 2\ln^2 \bar{u} \right) \text{Li}_2(u) - \frac{3}{4} \ln^4 u + \frac{7}{3} \ln^3 u \ln \bar{u} \\
& - \frac{1}{2} \ln^2 u \ln^2 \bar{u} - \frac{1}{3} \ln u \ln^3 \bar{u} + \frac{3}{4} \ln^4 \bar{u} - \frac{4-11u+3u^2}{u\bar{u}} \text{Li}_3(u) + \frac{5-12u}{6\bar{u}} \ln^3 u \\
& + \frac{1+u-3u^2}{u\bar{u}} \text{S}_{1,2}(u) + \frac{2-10u+6u^2}{u\bar{u}} \ln u \text{Li}_2(u) - \frac{1-5u+3u^2}{u\bar{u}} \ln \bar{u} \text{Li}_2(u) \\
& + \frac{2-10u+9u^2}{2u\bar{u}} \ln^2 u \ln \bar{u} - \frac{1-2u}{2u\bar{u}} \ln u \ln^2 \bar{u} - \frac{5-6u}{6u} \ln^3 \bar{u} \\
& - \frac{18-24u+15u^2-10u\bar{u}\pi^2}{3u\bar{u}} \text{Li}_2(u) - \frac{16-27u+4\bar{u}\pi^2}{4\bar{u}} \ln^2 u \\
& - \frac{6-36u+27u^2-4u\bar{u}\pi^2}{2u\bar{u}} \ln u \ln \bar{u} + \frac{3(14-17u)+8u\pi^2}{12u} \ln^2 \bar{u} \\
& + \frac{8-15u-4\pi^2-48\bar{u}\zeta_3}{4\bar{u}} \ln u + \frac{3(2-3u)\zeta_3}{\bar{u}} - \frac{23\pi^4}{60} + \frac{(23-17u)\pi^2}{12\bar{u}} \\
& - \frac{81-126u+45u^2-(14-22u+6u^2)\pi^2-192u\bar{u}\zeta_3}{12u\bar{u}} \ln \bar{u} - \frac{137}{4},
\end{aligned}$$

$$t_{E,2}(u) = -\frac{6(1-2u)}{u\bar{u}}\text{Li}_2(u) - \frac{6}{u}\ln u \ln \bar{u} - 6\ln u - 6\ln \bar{u} - \frac{\pi^2}{\bar{u}} + 50. \quad (42)$$

In the calculation of the colour-suppressed tree amplitude, the NLO kernels in (22) contain the coefficient functions

$$\begin{aligned} \hat{t}_1(u) &= \frac{u}{\bar{u}}\ln u - \ln \bar{u} + 8 + i\pi, \\ \hat{t}_2(u) &= \frac{u}{\bar{u}}\left(\text{Li}_2(u) - \ln^2 u + \ln u \ln \bar{u} + 4\ln u\right) + \frac{1}{2}\ln^2 \bar{u} - 4\ln \bar{u} - \frac{(3-2u)\pi^2}{6\bar{u}} + 20 \\ &\quad + i\pi(4 - \ln \bar{u}), \\ \hat{t}_{E,0}(u) &= \frac{\bar{u}}{u}\ln \bar{u} - \ln u + 6 + i\pi, \\ \hat{t}_{E,1}(u) &= -\frac{\bar{u}}{u}\left(\text{Li}_2(u) + \ln^2 \bar{u} - 3\ln \bar{u}\right) + \frac{1}{2}\ln^2 u - 3\ln u + 14 - \frac{\pi^2}{2} + i\pi(3 - \ln u) \end{aligned} \quad (43)$$

and the convolutions with the NLO kernels, cf. (25) and (26), give rise to

$$\begin{aligned} \hat{t}_3(u) &= \frac{\pi^2}{3} - 5 + \frac{u}{\bar{u}}\ln^2 u + 2\ln u \ln \bar{u} - \ln^2 \bar{u} - \frac{\ln \bar{u}}{u}, \\ \hat{t}_{E,2}(u) &= \frac{1}{\bar{u}}\left(6\text{Li}_2(u) + 3u\ln u - \pi^2\right) - \frac{3(1+u)}{u}\ln \bar{u} + 27 + 3i\pi, \\ \hat{t}_{F,0}(u) &= \frac{1}{\bar{u}}\left(2(1+2u)\text{Li}_2(u) - u\ln^2 u - 2\bar{u}\ln u \ln \bar{u} + 3u\ln u - (2+u)\frac{\pi^2}{3}\right) \\ &\quad + \frac{\bar{u}}{u}\ln^2 \bar{u} - \frac{3(1+u)}{u}\ln \bar{u} + 29 + i\pi\left(3 - \frac{2u}{\bar{u}}\ln u + \frac{2\bar{u}}{u}\ln \bar{u}\right). \end{aligned} \quad (44)$$

B Calculation of 2-loop counterterms $\hat{\Delta}_{F,i}^{(2)}$

We present the calculation of the 2-loop counterterms $\hat{\Delta}_{F,i}^{(2)}$, that are required in the NNLO calculation of the colour-suppressed tree amplitude as described in Section 2.4. The counterterms receive three contributions

$$\hat{\Delta}_{F,i}^{(2)} = \hat{T}_{i,F}^{(0)} \otimes \left\{ \hat{F}_F^{(2)} \hat{\Phi}_F^{(0)} + \hat{F}_F^{(1)} \hat{\Phi}_F^{(1)} + \hat{F}_F^{(0)} \hat{\Phi}_F^{(2)} \right\}_{\text{ct}} \quad (45)$$

where \otimes represents a convolution and "ct" refers to the counterterm contributions of the form factor and the wave function corrections. Notice that the wave function corrections actually correspond to local corrections to the decay constant, as a consequence of the fact that the tree level kernels $\hat{T}_{i,F}^{(0)}$ are constant (cf. also (20) and (21)).

We first consider the mixed term $\hat{F}_F^{(1)} \hat{\Phi}_F^{(1)}$, which involves the calculation of the diagrams from Figure 3. The first diagram vanishes due to a scaleless loop integral and the

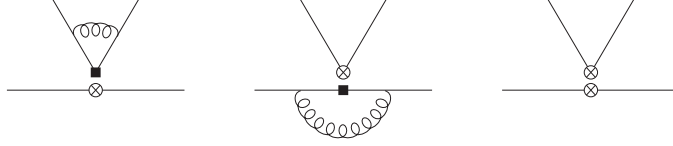


Figure 3: *Diagrams that contribute to the mixed contribution $\hat{F}_F^{(1)} \hat{\Phi}_F^{(1)}$. The symbol \otimes in the lower (upper) line refers to an insertion of the 1-loop counter-term from the form factor (wave function) correction of the operator $\tilde{\mathcal{O}}_F$.*

second diagram yields

$$\delta_1 = -C_F^2 \left(\frac{e^{\gamma_E} \mu^2}{m_b^2} \right)^\varepsilon \Gamma(\varepsilon) \left\{ \left(\frac{1 - \varepsilon + 2\varepsilon^2}{\varepsilon(1 - 2\varepsilon)} + \frac{6(1 + \varepsilon)}{(1 - \varepsilon)^2} \right) \hat{F}^{(0)} \hat{\Phi}^{(0)} + \frac{6(1 + \varepsilon)}{(1 - \varepsilon)^2} \hat{F}_F^{(0)} \hat{\Phi}_F^{(0)} \right. \\ \left. + \frac{1 - 6\varepsilon + 16\varepsilon^2 - 14\varepsilon^3}{4\varepsilon^2(1 - 2\varepsilon)(1 - \varepsilon)^2} \hat{F}_E^{(0)} \hat{\Phi}_E^{(0)} + \frac{1}{16\varepsilon(1 - \varepsilon)^2} \hat{F}_{E'}^{(0)} \hat{\Phi}_{E'}^{(0)} \right\}. \quad (46)$$

We are left with the 2-loop counterterm from the last diagram of Figure 3, which requires the calculation of the UV-divergences of the 2-loop diagram from Figure 4. For this it is convenient to apply the method proposed in [25] (sometimes called *IR-rearrangement*), which allows to set all masses and external momenta to zero. The calculation then reduces to the evaluation of 2-loop tadpole integrals, which depend on a single mass scale (an artificial scale that has been introduced to separate UV- and IR-divergences). Computing the 1-loop counterterms with the same prescription and accounting for the wave-function renormalization, we get

$$\delta_2 = C_F^2 \left\{ \left(\frac{6}{\varepsilon} + 5 \right) \hat{F}^{(0)} \hat{\Phi}^{(0)} - \left(\frac{3}{4\varepsilon^2} - \frac{1}{\varepsilon} \right) \hat{F}_E^{(0)} \hat{\Phi}_E^{(0)} + \frac{1}{16\varepsilon^2} \hat{F}_{E'}^{(0)} \hat{\Phi}_{E'}^{(0)} + \frac{6}{\varepsilon} \hat{F}_F^{(0)} \hat{\Phi}_F^{(0)} \right\}. \quad (47)$$

Next we compute the form factor correction $\hat{F}_F^{(2)} \hat{\Phi}_F^{(0)}$ (the corresponding diagrams are shown in Figure 5a). The first diagram gives again the contribution δ_1 from (46). On the other hand the computation of the 2-loop counterterm from the second diagram of Figure 5a is rather involved. It requires the calculation of the UV-divergences of a couple of 2-loop diagrams (shown e.g. in Figure 1 of [15]) and the corresponding 1-loop counterterms. Proceeding as before with the method of *IR-rearrangement* and accounting for the 2-loop wave-function renormalization in the $\overline{\text{MS}}$ -scheme [26],

$$Z_{2,b}^{(2)} = Z_{2,q}^{(2)} = C_F \left\{ \left(\frac{1}{2} C_F + C_A \right) \frac{1}{\varepsilon^2} + \left(\frac{3}{4} C_F - \frac{17}{4} C_A + \frac{1}{2} n_f \right) \frac{1}{\varepsilon} \right\}, \quad (48)$$

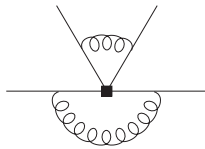


Figure 4: *The UV-divergences of this 2-loop diagram contribute to δ_2 .*

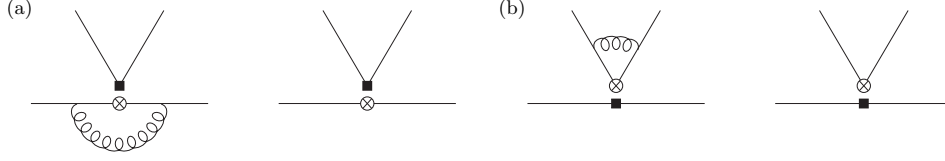


Figure 5: *Diagrams that contribute to $\hat{F}_F^{(2)} \hat{\Phi}_F^{(0)}$ (a) and $\hat{F}_F^{(0)} \hat{\Phi}_F^{(2)}$ (b).*

yields the 2-loop form factor counterterm for the Fierz-evanescent operator $\tilde{\mathcal{O}}_F$ ¹⁵

$$\begin{aligned} \delta_3 = C_F \Big\{ & \left[\left(3C_F - \frac{11}{6}C_A + \frac{1}{3}n_f \right) \frac{1}{\varepsilon} + \left(-\frac{17}{2}C_F + \frac{149}{36}C_A + \frac{5}{18}n_f \right) \right] \hat{F}_F^{(0)} \hat{\Phi}_F^{(0)} \\ & + \left[\left(-\frac{3}{8}C_F - \frac{11}{24}C_A + \frac{1}{12}n_f \right) \frac{1}{\varepsilon^2} + \left(\frac{9}{16}C_F + \frac{53}{144}C_A - \frac{1}{72}n_f \right) \frac{1}{\varepsilon} \right] \hat{F}_E^{(0)} \hat{\Phi}_E^{(0)} \\ & + \left[\frac{C_F}{32\varepsilon^2} + \left(-\frac{5}{64}C_F + \frac{1}{32}C_A \right) \frac{1}{\varepsilon} \right] \hat{F}_{E'}^{(0)} \hat{\Phi}_{E'}^{(0)} + \left(3C_F - \frac{11}{6}C_A + \frac{1}{3}n_f \right) \frac{1}{\varepsilon} \hat{F}_F^{(0)} \hat{\Phi}_F^{(0)} \Big\}. \end{aligned} \quad (49)$$

We finally account for the wave function correction $\hat{F}_F^{(0)} \hat{\Phi}_F^{(2)}$ from Figure 5b. The first diagram again vanishes due to a scaleless integral and the second diagram yields, in a convolution with a constant kernel, again the contribution δ_3 from (49).

To summarize, in terms of the individual contributions δ_i from (46), (47) and (49), the 2-loop counterterms required in the calculation of the colour-suppressed amplitude become

$$\hat{\Delta}_{F,1}^{(2)} = C_F \hat{\Delta}_{F,2}^{(2)} = \frac{C_F}{N_C} \left\{ 2\delta_1 + \delta_2 + 2\delta_3 \right\}. \quad (50)$$

C NNLO hard-scattering kernels

Our final expressions for the real parts of the NNLO vertex corrections from (31) involve the following set of hard-scattering kernels,

$$\begin{aligned} h_5(u) = & \left[\frac{4(3 - 3u + 8u^2 - 2u^3)}{\bar{u}^3} \text{Li}_4(u) - \frac{8(12 - 35u + 36u^2 - 14u^3 + 4u^4)}{u^3 \bar{u}^2} \text{S}_{2,2}(u) \right. \\ & - 24 \ln u \text{Li}_3(u) - \frac{8(12 - 47u + 71u^2 - 48u^3 + 24u^4)}{u^3 \bar{u}^3} \left(\ln \bar{u} \text{Li}_3(u) - \zeta_3 \ln u \right) \\ & + \frac{17 - 82u^2 + 40u^4 - 16u^6}{2u^3 \bar{u}^3} \text{Li}_2(u)^2 + 4 \ln^2 u \text{Li}_2(u) + \frac{2}{3} \ln^4 u - \frac{4}{3} \ln^3 u \ln \bar{u} \\ & \left. - \frac{122 - 91u^2 + 20u^4}{3u \bar{u}^3} \ln u \ln \bar{u} \text{Li}_2(u) - \frac{51 + 16u^2 + 268u^4 + 4u^6}{12u^3 \bar{u}^3} \ln^2 u \ln^2 \bar{u} \right] \end{aligned}$$

¹⁵We performed this calculation for arbitrary bilinear quark currents, which allows us to perform several cross-checks. We in particular verified that the anomalous dimension of the vector current vanishes at the 2-loop level and reproduced the one of the scalar and the tensor current from [27].

$$\begin{aligned}
& + \frac{3 - 108u + 351u^2 - 440u^3 + 266u^4 - 74u^5 + 17u^6 - 16u^7 + 4u^8}{u^3 \bar{u}^3} \text{Li}_3(u) \\
& - \frac{3 - 78u + 109u^2 - 43u^3 - 6u^4}{u^3 \bar{u}} \ln u \text{Li}_2(u) - \frac{u(3 - 3u + 2u^2)}{6\bar{u}} \ln^3 u \\
& - \frac{3 - 54u + 69u^2 - 18u^3 - 6u^4 + 3u^5 - 2u^6}{2u^3 \bar{u}} \ln^2 u \ln \bar{u} \\
& + \frac{3 - 3u - 7u^2 - 3u^3}{u^3} \left(\text{Li}_3(-u) - \ln u \text{Li}_2(-u) - \frac{\ln^2 u + \pi^2}{2} \ln(1 + u) \right) \\
& - \frac{(\bar{u} - u)(6(5 - 66u^2 + 60u^4 - 4u^6) + 4(19 - 91u^2 - 2u^4)\pi^2)}{24u^3 \bar{u}^3} \text{Li}_2(u) \\
& + \left(\frac{42 - 57u - 22u^2 + 49u^3 - 4u^4}{4u\bar{u}^2} - 2\pi^2 \right) \ln^2 u \\
& + \left(\frac{273 - 535u + 302u^4 - 90u^5}{40u^2 \bar{u}^3} + \frac{(701 - 55u + 2794u^4 - 620u^5)\pi^2}{180u^2 \bar{u}^3} \right) \ln u \ln \bar{u} \\
& - \left(\frac{167 - 302u}{4\bar{u}} - \frac{(96 - 160u + 59u^2 + 9u^3 + 3u^4 - 2u^5)\pi^2}{6u^2 \bar{u}} \right) \ln u \\
& + \frac{(849 - 3456u + 4496u^2 - 2408u^3 + 2024u^4 - 984u^5 + 328u^6)\pi^4}{720u^3 \bar{u}^3} \\
& + \frac{(5 - 262u + 938u^2 - 1582u^3 + 1366u^4 - 690u^5 + 230u^6)\pi^2}{48u^3 \bar{u}^3} + \frac{1507}{8} \\
& - \frac{(3 - 110u + 358u^2 - 424u^3 + 32u^4 + 216u^5 - 72u^6)\zeta_3}{2u^3 \bar{u}^3} + (u \leftrightarrow \bar{u}) \Big] \\
& + \left[- \frac{8(1 + 2u)}{\bar{u}^3} \text{Li}_4(u) - \frac{8(12 - 35u + 36u^2 - 14u^3 + 4u^4)}{u^3 \bar{u}^2} \text{S}_{2,2}(u) \right. \\
& - \frac{(\bar{u} - u)(12 - 23u + 25u^2 - 4u^3 + 2u^4)}{u^3 \bar{u}^3} \left(8 \ln \bar{u} \text{Li}_3(u) + \ln^2 u \ln^2 \bar{u} - 8\zeta_3 \ln u \right) \\
& - \frac{2(\bar{u} - u)(3 - 5u + 5u^2)}{u^3 \bar{u}^3} \text{Li}_2(u)^2 - \frac{3 - 72u + 85u^2 - 9u^3 + 18u^4}{u^3 \bar{u}} \ln u \text{Li}_2(u) \\
& - \frac{2(3 - 11u + 15u^2 - 8u^3 + 4u^4)}{u^3 \bar{u}^3} \left(\ln u \ln \bar{u} - \frac{7\pi^2}{6} \right) \text{Li}_2(u) \\
& + \frac{3 - 102u + 293u^2 - 278u^3 + 36u^4 + 74u^5 - 43u^6 + 14u^7}{u^3 \bar{u}^3} \text{Li}_3(u) \\
& - \frac{12 - 25u + 7u^2}{6\bar{u}} \ln^3 u - \frac{3 - 48u + 57u^2 - 6u^3 + 16u^4 - 7u^5}{2u^3 \bar{u}} \ln^2 u \ln \bar{u} \\
& + \frac{3 + 3u + 5u^2 + 3u^3}{u^3} \left(\text{Li}_3(-u) - \ln u \text{Li}_2(-u) - \frac{\ln^2 u + \pi^2}{2} \ln(1 + u) \right)
\end{aligned}$$

$$\begin{aligned}
& + \frac{21 - 62u - 29u^2 + 182u^3 - 91u^4}{2u^2\bar{u}^2} \text{Li}_2(u) + \frac{42 + u - 142u^2 + 91u^3}{4u\bar{u}^2} \ln^2 u \\
& + \frac{(\bar{u} - u)(3u\bar{u}(21 - 13u + 13u^2) + 4(33 - 61u + 65u^2 - 8u^3 + 4u^4)\pi^2)}{12u^3\bar{u}^3} \ln u \ln \bar{u} \\
& - \frac{111u^2 - 2(96 - 112u - 29u^2 + 37u^3 - 7u^4)\pi^2}{12u^2\bar{u}} \ln u \\
& + \frac{(\bar{u} - u)(48 - 83u + 85u^2 - 4u^3 + 2u^4)\pi^4}{90u^3\bar{u}^3} - \frac{(\bar{u} - u)(147 - 74u + 74u^2)\pi^2}{24u^2\bar{u}^2} \\
& - \frac{(\bar{u} - u)(3 - 110u + 96u^2 + 28u^3 - 14u^4)\zeta_3}{2u^3\bar{u}^3} - (u \leftrightarrow \bar{u}) \Big], \\
h_6(u) = & \left[\frac{327}{2} - \frac{3(1 - 2u)}{2\bar{u}} \ln^2 u + \frac{3(1 - 2u^2)}{2u\bar{u}} \ln u \ln \bar{u} - \frac{3(13 - 24u)}{2\bar{u}} \ln u \right. \\
& \left. + \frac{(1 - 2u^2)\pi^2}{4u\bar{u}} + (u \leftrightarrow \bar{u}) \right] \\
& + \left[8\text{Li}_3(u) - 8 \ln u \text{Li}_2(u) + \frac{4}{3} \ln^3 u - 4 \ln^2 u \ln \bar{u} - \frac{13 - 24u^2}{u\bar{u}} \text{Li}_2(u) \right. \\
& \left. + \frac{25 - 24u}{2\bar{u}} \ln^2 u + \frac{13}{\bar{u}} \ln u \ln \bar{u} - \frac{9}{2\bar{u}} \ln u - \frac{11\pi^2}{6\bar{u}} - (u \leftrightarrow \bar{u}) \right], \\
h_7(u) = & \left[\frac{(1 + u)(3 - 4u + 3u^2)}{3u\bar{u}^2} \left(12\mathcal{H}_1(u) + \pi^2 \ln(1 + u) \right) - 48 \ln u \text{Li}_3(u) \right. \\
& + \frac{2u}{3\bar{u}^3} \left(24\mathcal{H}_2(u) - 2\pi^2 \text{Li}_2(-u) \right) + \frac{4(6 - 9u + 16u^2 - 4u^3)}{\bar{u}^3} \text{Li}_4(u) + 8 \ln^2 u \text{Li}_2(u) \\
& - \frac{4(52 - 152u + 156u^2 - 61u^3 + 18u^4 - u^5)}{u^3\bar{u}^2} \text{S}_{2,2}(u) + \frac{4}{3} \ln^4 u - \frac{8}{3} \ln^3 u \ln \bar{u} \\
& - \frac{4(52 - 204u + 308u^2 - 209u^3 + 107u^4 - 3u^5 + u^6)}{u^3\bar{u}^3} \left(\ln \bar{u} \text{Li}_3(u) - \zeta_3 \ln u \right) \\
& - \frac{13 - 54u + 88u^2 - 84u^3 + 82u^4 - 48u^5 + 16u^6}{u^3\bar{u}^3} \text{Li}_2(u)^2 + \frac{3 - 18u + 6u^2 - 4u^3}{6\bar{u}} \ln^3 u \\
& - \frac{(\bar{u} - u)(1 - 2u + 2u^2)(13 - 2u + 2u^2)}{u^3\bar{u}^3} \ln u \ln \bar{u} \text{Li}_2(u) \\
& - \frac{6 - 168u + 235u^2 - 107u^3 - 6u^4}{u^3\bar{u}} \ln u \text{Li}_2(u) \\
& - \frac{52 - 204u + 308u^2 - 197u^3 + 71u^4 + 33u^5 - 11u^6}{2u^3\bar{u}^3} \ln^2 u \ln^2 \bar{u} \\
& \left. + \frac{2(3 - 116u + 374u^2 - 465u^3 + 280u^4 - 78u^5 + 17u^6 - 16u^7 + 4u^8)}{u^3\bar{u}^3} \text{Li}_3(u) \right]
\end{aligned}$$

$$\begin{aligned}
& - \frac{6 - 116u + 149u^2 - 50u^3 - 6u^4 + 6u^5 - 4u^6}{2u^3\bar{u}} \ln^2 u \ln \bar{u} \\
& + \frac{2(3 - 3u - 7u^2 - 3u^3)}{u^3} \left(\text{Li}_3(-u) - \ln u \text{Li}_2(-u) - \frac{\ln^2 u + \pi^2}{2} \ln(1 + u) \right) + (\bar{u} - u) \\
& \times \left(\frac{92 - 117u + 109u^2 + 16u^3 - 8u^4}{4u^2\bar{u}^2} + \frac{(1 - 2u + 2u^2)(83 - 14u + 14u^2)\pi^2}{6u^3\bar{u}^3} \right) \text{Li}_2(u) \\
& + \left(\frac{46 - 73u + 26u^2 + 13u^3 - 4u^4}{2u\bar{u}^2} - 4\pi^2 \right) \ln^2 u + \left(\frac{92 - 289u + 421u^2 - 264u^3 + 132u^4}{4u\bar{u}^2} \right. \\
& + \left. \frac{(139 - 554u + 856u^2 - 558u^3 + 164u^4 + 138u^5 - 46u^6)\pi^2}{3u^2\bar{u}^3} \right) \ln u \ln \bar{u} \\
& - \left(\frac{183 - 308u}{2\bar{u}} - \frac{(96 - 160u + 55u^2 + 15u^3 + 3u^4 - 2u^5)\pi^2}{3u^2\bar{u}} \right) \ln u \\
& + \frac{(191 - 784u + 1262u^2 - 1121u^3 + 973u^4 - 495u^5 + 165u^6)\pi^4}{180u^3\bar{u}^3} \\
& - \frac{(580 - 1763u + 2239u^2 - 952u^3 + 476u^4)\pi^2}{48u^2\bar{u}^2} \\
& - \left. \frac{3(1 - 37u + 119u^2 - 138u^3 + 4u^4 + 78u^5 - 26u^6)\zeta_3}{u^3\bar{u}^3} + \frac{1659}{4} + (u \leftrightarrow \bar{u}) \right] \\
& + \left[\frac{(1 + u)(1 + 4u - 7u^2)}{3u\bar{u}^2} \left(12\mathcal{H}_1(u) + \pi^2 \ln(1 + u) \right) - 36 \ln u \text{Li}_3(u) + 14 \ln^2 u \text{Li}_2(u) \right. \\
& + \frac{2(1 - 4u + 3u^2 - u^3)}{3\bar{u}^3} \left(24\mathcal{H}_2(u) - 2\pi^2 \text{Li}_2(-u) \right) + \frac{4(2 - 23u + 18u^2 - 6u^3)}{\bar{u}^3} \text{Li}_4(u) \\
& - \frac{4(52 - 152u + 156u^2 - 61u^3 + 18u^4 - u^5)}{u^3\bar{u}^2} \text{S}_{2,2}(u) - \frac{(\bar{u} - u)(13 - 22u\bar{u})}{u^3\bar{u}^3} \text{Li}_2(u)^2 \\
& - \frac{2(13 - 51u + 77u^2 - 59u^3 + 13u^4 - 7u^5 + u^6)}{u^3\bar{u}^3} \left(8 \ln \bar{u} \text{Li}_3(u) + \ln^2 u \ln^2 \bar{u} - 8\zeta_3 \ln u \right) \\
& - \frac{13 - 48u + 66u^2 - 30u^3 + 18u^5 - 6u^6}{u^3\bar{u}^3} \left(\ln u \ln \bar{u} - \frac{7\pi^2}{6} \right) \text{Li}_2(u) - \ln^4 u + \frac{8}{3} \ln^3 u \ln \bar{u} \\
& + \frac{2(3 - 110u + 339u^2 - 362u^3 + 100u^4 + 59u^5 - 46u^6 + 14u^7)}{u^3\bar{u}^3} \text{Li}_3(u) \\
& - \frac{6 - 156u + 227u^2 - 57u^3 + 38u^4}{u^3\bar{u}} \ln u \text{Li}_2(u) - \frac{9 - 32u + 14u^2}{6\bar{u}} \ln^3 u \\
& - \frac{6 - 104u + 165u^2 - 54u^3 + 34u^4 - 14u^5}{2u^3\bar{u}} \ln^2 u \ln \bar{u} \\
& + \left. \frac{2(3 + 3u + 5u^2 + 3u^3)}{u^3} \left(\text{Li}_3(-u) - \ln u \text{Li}_2(-u) - \frac{\ln^2 u + \pi^2}{2} \ln(1 + u) \right) \right]
\end{aligned}$$

$$\begin{aligned}
& + \left(\frac{92 - 381u + 161u^2 + 440u^3 - 220u^4}{4u^2\bar{u}^2} - \frac{4(1 - 3u + 3u^2)(\bar{u} + 2u^3 - u^4)\pi^2}{3u^3\bar{u}^3} \right) \text{Li}_2(u) \\
& + \left(\frac{46 - 47u - 62u^2 + 55u^3}{2u\bar{u}^2} - \frac{4\pi^2}{3} \right) \ln^2 u + \frac{(\bar{u} - u)(13 + 169u^2 - 8u^3 + 4u^4)\pi^4}{90u^3\bar{u}^3} \\
& + \left(\frac{(1 + u)(246 - 169u^2)}{4u^2\bar{u}^2} + \frac{(87 - 210u^2 - 16u^4)\pi^2}{3u^2\bar{u}^3} \right) \ln u \ln \bar{u} \\
& - \left(\frac{93}{6\bar{u}} - \frac{(96 - 112u - 31u^2 + 34u^3 - 7u^4)\pi^2}{3u^2\bar{u}} + 4\zeta_3 \right) \ln u \\
& - \frac{(\bar{u} - u)(580 - 187u + 187u^2)\pi^2}{48u^2\bar{u}^2} + \frac{8(\bar{u} - u)\pi^2}{u\bar{u}} \ln 2 \\
& - \frac{3(\bar{u} - u)(1 - 39u + 42u^2 - 6u^3 + 3u^4)\zeta_3}{u^3\bar{u}^3} - (u \leftrightarrow \bar{u}) \Big], \\
h_8(u) = & \left[- \frac{(1 + u)(3 - 4u + 3u^2)}{6u\bar{u}^2} \left(12\mathcal{H}_1(u) + \pi^2 \ln(1 + u) \right) + 18 \ln u \text{Li}_3(u) \right. \\
& - \frac{u}{3\bar{u}^3} \left(24\mathcal{H}_2(u) - 2\pi^2 \text{Li}_2(-u) \right) - \frac{5 - 22u + 20u^2 - 6u^3}{\bar{u}^3} \text{Li}_4(u) - 3 \ln^2 u \text{Li}_2(u) \\
& + \frac{4(5 - 11u + 5u^2 + 5u^3 + 4u^4 - u^5)}{u^3\bar{u}^2} \text{S}_{2,2}(u) - \frac{1}{2} \ln^4 u + \ln^3 u \ln \bar{u} \\
& + \frac{4(5 - 16u + 16u^2 - u^3 + 3u^4 - 3u^5 + u^6)}{u^3\bar{u}^3} \left(\ln \bar{u} \text{Li}_3(u) - \zeta_3 \ln u \right) \\
& + \frac{(\bar{u} - u)^2(5 - 3u + 9u^2 - 12u^3 + 6u^4)}{4u^3\bar{u}^3} \text{Li}_2(u)^2 + \frac{3 + u - 3u^2 + 2u^3}{6\bar{u}} \ln^3 u \\
& + \frac{(\bar{u} - u)(5 - 13u + 15u^2 - 4u^3 + 2u^4)}{4u^3\bar{u}^3} \ln u \ln \bar{u} \text{Li}_2(u) \\
& + \frac{10 - 32u + 32u^2 + 7u^3 - 21u^4 + 21u^5 - 7u^6}{4u^3\bar{u}^3} \ln^2 u \ln^2 \bar{u} \\
& - \frac{6 - 61u + 157u^2 - 196u^3 + 134u^4 - 42u^5 + 32u^6 - 32u^7 + 8u^8}{2u^3\bar{u}^3} \text{Li}_3(u) \\
& + \frac{6 - 39u + 47u^2 - 35u^3 - 12u^4}{2u^3\bar{u}} \ln u \text{Li}_2(u) - \frac{(4 + 35u - 254u^2 + 438u^3 - 219u^4)\pi^2}{48u^2\bar{u}^2} \\
& + \frac{(2 - u + u^2)(3 - 13u + 5u^2 + 2u^3 - 4u^4)}{4u^3\bar{u}} \ln^2 u \ln \bar{u} \\
& - \frac{6 - 3u - 8u^2 - 3u^3}{2u^3} \left(\text{Li}_3(-u) - \ln u \text{Li}_2(-u) - \frac{\ln^2 u + \pi^2}{2} \ln(1 + u) \right) - (\bar{u} - u) \\
& \times \left(\frac{(4 - 7u + 2u^2)(1 - 3u - 2u^2)}{4u^2\bar{u}^2} + \frac{(19 - 59u + 73u^2 - 28u^3 + 14u^4)\pi^2}{24u^3\bar{u}^3} \right) \text{Li}_2(u)
\end{aligned}$$

$$\begin{aligned}
& - \left(\frac{8 + 37u - 136u^2 + 115u^3 - 8u^4}{8u\bar{u}^2} - \frac{3\pi^2}{2} \right) \ln^2 u \\
& - \left(\frac{4 - 3u + 24u^2 - 42u^3 + 21u^4}{8u^2\bar{u}^2} + \frac{(127 - 590u^2 + 652u^4 - 128u^6)\pi^2}{48u^3\bar{u}^3} \right) \ln u \ln \bar{u} \\
& + \left(\frac{1433 - 2710u}{24\bar{u}} - \frac{(12 - 30u + 8u^2 + 11u^3 + 3u^4 - 2u^5)\pi^2}{6u^2\bar{u}} \right) \ln u \\
& - \frac{(23 - 102u + 176u^2 - 273u^3 + 449u^4 - 375u^5 + 125u^6)\pi^4}{360u^3\bar{u}^3} \\
& + \left[\frac{(6 - 57u + 134u^2 + 26u^3 - 463u^4 + 540u^5 - 180u^6)\zeta_3}{4u^3\bar{u}^3} - \frac{12641}{48} + (u \leftrightarrow \bar{u}) \right] \\
& + \left[- \frac{(1+u)(1+4u-7u^2)}{6u\bar{u}^2} \left(12\mathcal{H}_1(u) + \pi^2 \ln(1+u) \right) + 2 \ln u \operatorname{Li}_3(u) - 3 \ln^2 u \operatorname{Li}_2(u) \right. \\
& - \frac{1-4u+3u^2-u^3}{3\bar{u}^3} \left(24\mathcal{H}_2(u) - 2\pi^2 \operatorname{Li}_2(-u) \right) + \frac{19-44u+36u^2-14u^3}{\bar{u}^3} \operatorname{Li}_4(u) \\
& + \frac{4(5-11u+5u^2+5u^3+4u^4-u^5)}{u^3\bar{u}^2} \operatorname{S}_{2,2}(u) + \frac{(\bar{u}-u)(\bar{u}+u^2)(5+6u-6u^2)}{4u^3\bar{u}^3} \operatorname{Li}_2(u)^2 \\
& + \frac{5-16u+16u^2-5u^3-7u^4+u^5+u^6}{2u^3\bar{u}^3} \left(8 \ln \bar{u} \operatorname{Li}_3(u) + \ln^2 u \ln^2 \bar{u} - 8\zeta_3 \ln u \right) \\
& + \frac{3-6u^2+36u^4-16u^6}{8u^3\bar{u}^3} \left(\ln u \ln \bar{u} - \frac{7\pi^2}{6} \right) \operatorname{Li}_2(u) - \frac{1}{12} \ln^4 u - \frac{2}{3} \ln^3 u \ln \bar{u} \\
& - \frac{(\bar{u}-u)(7-4u-20u^2+48u^3-24u^4)}{16u^3\bar{u}^3} \ln^2 u \ln^2 \bar{u} \\
& - \frac{18-165u+237u^2+242u^3-702u^4+546u^5-278u^6+84u^7}{6u^3\bar{u}^3} \operatorname{Li}_3(u) \\
& + \frac{6-33u+19u^2+7u^3+48u^4}{2u^3\bar{u}} \ln u \operatorname{Li}_2(u) + \frac{30-42u+7u^2}{6\bar{u}} \ln^3 u \\
& + \frac{18-69u+78u^2-124u^3+217u^4-42u^5}{12u^3\bar{u}} \ln^2 u \ln \bar{u} \\
& - \frac{6+3u+4u^2+3u^3}{2u^3} \left(\operatorname{Li}_3(-u) - \ln u \operatorname{Li}_2(-u) - \frac{\ln^2 u + \pi^2}{2} \ln(1+u) \right) \\
& - \frac{(\bar{u}-u)(6-283u+283u^2)\pi^2}{72u^2\bar{u}^2} - \left(\frac{36-312u-1493u^2+3610u^3-1805u^4}{36u^2\bar{u}^2} \right. \\
& - \left. \frac{(2-8u+12u^2-5u^3-5u^4+9u^5-3u^6)\pi^2}{3u^3\bar{u}^3} \right) \operatorname{Li}_2(u) - \frac{4(\bar{u}-u)\pi^2}{u\bar{u}} \ln 2 \\
& - \left(\frac{72+1703u-3724u^2+1805u^3}{72u\bar{u}^2} + \frac{\pi^2}{3} \right) \ln^2 u
\end{aligned}$$

$$\begin{aligned}
& - \left(\frac{(\bar{u} - u)(3 - 10u + 10u^2)}{6u^2\bar{u}^2} - \frac{(33 - 21u + 35u^2 - 28u^3 + 14u^4)\pi^2}{12u^2\bar{u}^3} \right) \ln u \ln \bar{u} \\
& + \left(\frac{1009}{72\bar{u}} - \frac{(12 + 26u - 121u^2 + 80u^3 - 7u^4)\pi^2}{6u^2\bar{u}} + 4\zeta_3 \right) \ln u \\
& - \frac{(\bar{u} - u)(429 + 84u - 1244u^2 + 2320u^3 - 1160u^4)\pi^4}{2880u^3\bar{u}^3} \\
& + \frac{3(\bar{u} - u)(2 - 21u - 4u^2 + 50u^3 - 25u^4)\zeta_3}{4u^3\bar{u}^3} - (u \leftrightarrow \bar{u}) \Big]. \tag{51}
\end{aligned}$$

The definition of the functions $\mathcal{H}_{1,2}(x)$ can be found in Section 2.2. The diagrams with a closed fermion loop give for massless internal quarks

$$\begin{aligned}
h_9(u; 0) = & \left[\frac{125}{12} + \frac{\text{Li}_2(u)}{\bar{u}} + \frac{1 - 3u}{2\bar{u}} \ln^2 u + \frac{1 + u}{2\bar{u}} \ln u \ln \bar{u} - \frac{17(1 - 2u)}{6\bar{u}} \ln u \right. \\
& \left. - \frac{(1 + u)\pi^2}{12\bar{u}} + (u \leftrightarrow \bar{u}) \right] \\
& + \left[\frac{4}{3} \text{Li}_3(u) - \frac{2}{3} \ln^3 u + \frac{4}{3} \ln^2 u \ln \bar{u} - \frac{32 - 29u}{9\bar{u}} \text{Li}_2(u) + \frac{35 - 29u}{18\bar{u}} \ln^2 u \right. \\
& \left. - \frac{1}{3\bar{u}} \ln u \ln \bar{u} - \frac{13 + 24\bar{u}\pi^2}{18\bar{u}} \ln u + \frac{\pi^2}{18\bar{u}} - (u \leftrightarrow \bar{u}) \right], \tag{52}
\end{aligned}$$

and for an internal b -quark

$$\begin{aligned}
h_9(u; 1) = & \left[\frac{8}{u^2} \left(\text{Li}_3(-x_b) - \text{S}_{1,2}(-x_b) - \ln(1 + x_b) \text{Li}_2(-x_b) - \frac{1}{12} \ln^3 \frac{x_b}{1 + x_b} \right. \right. \\
& \left. - \frac{1}{6} \ln^3(1 + x_b) + \frac{\pi^2}{6} \ln \frac{x_b}{1 + x_b} \right) - \frac{14 - 75u^2 + 60u^4 + 19u^6}{9u^3\bar{u}^3} \ln u \ln \bar{u} \\
& - \frac{2y_b(6 + u)}{u} \left(\text{Li}_2(-x_b) - \frac{1}{4} \ln^2 \frac{x_b}{1 + x_b} + \frac{1}{2} \ln^2(1 + x_b) + \frac{\pi^2}{6} \right) + \frac{4u}{\bar{u}^3} \text{Li}_3(u) \\
& - \frac{32 - 204u + 504u^2 - 584u^3 + 405u^4 - 150u^5 + 29u^6}{9u^3\bar{u}^3} \text{Li}_2(u) - \frac{17(\bar{u} - u)}{6\bar{u}} \ln u \\
& - \frac{(40 - 213u^2 + 120u^4 - 19u^6)\pi^2}{54u^3\bar{u}^3} - \frac{2(1 - 6u^2 + 6u^4)\zeta_3}{u^3\bar{u}^3} \\
& \left. + \frac{5(61 - 50u^2)}{24u\bar{u}} + (u \leftrightarrow \bar{u}) \right] \\
& + \left[- \frac{8(3 - u^2)}{3u^2} \left(\text{Li}_3(-x_b) - \text{S}_{1,2}(-x_b) - \ln(1 + x_b) \text{Li}_2(-x_b) - \frac{1}{12} \ln^3 \frac{x_b}{1 + x_b} \right. \right. \\
& \left. - \frac{1}{6} \ln^3(1 + x_b) + \frac{\pi^2}{6} \ln \frac{x_b}{1 + x_b} \right) + \frac{54 - 103u^2 + 81u^4}{9u^2\bar{u}^3} \ln u \ln \bar{u}
\end{aligned}$$

$$\begin{aligned}
& + \frac{2y_b(38 + 29u)}{9u} \left(\text{Li}_2(-x_b) - \frac{1}{4} \ln^2 \frac{x_b}{1 + x_b} + \frac{1}{2} \ln^2(1 + x_b) + \frac{\pi^2}{6} \right) \\
& - \frac{4(1 + 3u^2 - u^3)}{3\bar{u}^3} \text{Li}_3(u) - \frac{128 - 504u + 389u^2}{18u^2\bar{u}} \ln u \\
& - \frac{32 - 204u + 504u^2 - 584u^3 + 405u^4 - 150u^5 + 29u^6}{9u^3\bar{u}^3} \text{Li}_2(u) \\
& + \frac{(42 - 49u + 39u^3)\pi^2}{54u\bar{u}^3} + \frac{4\zeta_3}{u^2\bar{u}^3} + \frac{261 - 325u^2}{9u\bar{u}^2} - (u \leftrightarrow \bar{u}) \Big], \tag{53}
\end{aligned}$$

where we introduced the shorthand notation

$$x_b = \frac{1}{2}(y_b - 1), \quad y_b = \sqrt{\frac{4 + u}{u}}. \tag{54}$$

We finally refrain from presenting the charm quark contribution, which is rather complicated and depends on two parameterizations for the 4-topology Master Integrals that we could not solve in a closed analytical form (cf. the discussion in [15]). We may still evaluate these Master Integrals numerically in Section 3.2 to perform the convolution with the light-cone distribution amplitude of the emitted meson M_2 .

References

- [1] M. Beneke, G. Buchalla, M. Neubert and C. T. Sachrajda, Phys. Rev. Lett. **83** (1999) 1914 [arXiv:hep-ph/9905312];
M. Beneke, G. Buchalla, M. Neubert and C. T. Sachrajda, Nucl. Phys. B **591** (2000) 313 [arXiv:hep-ph/0006124];
M. Beneke, G. Buchalla, M. Neubert and C. T. Sachrajda, Nucl. Phys. B **606** (2001) 245 [arXiv:hep-ph/0104110].
- [2] C. W. Bauer, S. Fleming, D. Pirjol and I. W. Stewart, Phys. Rev. D **63** (2001) 114020 [arXiv:hep-ph/0011336];
C. W. Bauer, D. Pirjol and I. W. Stewart, Phys. Rev. D **65** (2002) 054022 [arXiv:hep-ph/0109045];
M. Beneke, A. P. Chapovsky, M. Diehl and T. Feldmann, Nucl. Phys. B **643** (2002) 431 [arXiv:hep-ph/0206152].
- [3] M. Beneke and S. Jager, Nucl. Phys. B **751** (2006) 160 [arXiv:hep-ph/0512351];
N. Kivel, JHEP **0705** (2007) 019 [arXiv:hep-ph/0608291];
V. Pilipp, PhD thesis, LMU München, 2007, arXiv:0709.0497 [hep-ph];
V. Pilipp, Nucl. Phys. B **794** (2008) 154 [arXiv:0709.3214 [hep-ph]].
- [4] M. Beneke and S. Jager, Nucl. Phys. B **768** (2007) 51 [arXiv:hep-ph/0610322];
A. Jain, I. Z. Rothstein and I. W. Stewart, arXiv:0706.3399 [hep-ph].
- [5] G. Bell, Nucl. Phys. B **795** (2008) 1 [arXiv:0705.3127 [hep-ph]].

- [6] G. Bell, PhD thesis, LMU München, 2006, arXiv:0705.3133 [hep-ph].
- [7] K. G. Chetyrkin, M. Misiak and M. Munz, Nucl. Phys. B **520** (1998) 279 [arXiv:hep-ph/9711280].
- [8] M. Gorbahn and U. Haisch, Nucl. Phys. B **713** (2005) 291 [arXiv:hep-ph/0411071].
- [9] A. J. Buras, M. Gorbahn, U. Haisch and U. Nierste, JHEP **0611** (2006) 002 [arXiv:hep-ph/0603079].
- [10] M. Gorbahn, private communication.
- [11] F. V. Tkachov, Phys. Lett. B **100** (1981) 65;
K. G. Chetyrkin and F. V. Tkachov, Nucl. Phys. B **192** (1981) 159.
- [12] R. Bonciani and A. Ferroglia, JHEP **0811** (2008) 065 [arXiv:0809.4687 [hep-ph]];
H. M. Asatrian, C. Greub and B. D. Pecjak, Phys. Rev. D **78** (2008) 114028 [arXiv:0810.0987 [hep-ph]].
- [13] M. Beneke, T. Huber and X. Q. Li, Nucl. Phys. B **811** (2009) 77 [arXiv:0810.1230 [hep-ph]].
- [14] E. Remiddi and J. A. M. Vermaseren, Int. J. Mod. Phys. A **15** (2000) 725 [arXiv:hep-ph/9905237].
- [15] G. Bell, Nucl. Phys. B **812** (2009) 264 [arXiv:0810.5695 [hep-ph]].
- [16] T. Huber, arXiv:0901.2133 [hep-ph].
- [17] P. Gambino, M. Gorbahn and U. Haisch, Nucl. Phys. B **673** (2003) 238 [arXiv:hep-ph/0306079].
- [18] A. V. Efremov and A. V. Radyushkin, Phys. Lett. B **94** (1980) 245;
G. P. Lepage and S. J. Brodsky, Phys. Rev. D **22** (1980) 2157.
- [19] T. Becher, M. Neubert and B. D. Pecjak, Nucl. Phys. B **619** (2001) 538 [arXiv:hep-ph/0102219];
C. N. Burrell and A. R. Williamson, Phys. Rev. D **73** (2006) 114004 [arXiv:hep-ph/0504024].
- [20] R. J. Hill, T. Becher, S. J. Lee and M. Neubert, JHEP **0407** (2004) 081 [arXiv:hep-ph/0404217];
M. Beneke and D. Yang, Nucl. Phys. B **736** (2006) 34 [arXiv:hep-ph/0508250].
- [21] S. J. Lee and M. Neubert, Phys. Rev. D **72** (2005) 094028 [arXiv:hep-ph/0509350].
- [22] T. Becher and R. J. Hill, JHEP **0410** (2004) 055 [arXiv:hep-ph/0408344];
G. G. Kirilin, arXiv:hep-ph/0508235.

- [23] C. Bobeth, M. Misiak and J. Urban, Nucl. Phys. B **574** (2000) 291 [arXiv:hep-ph/9910220].
- [24] O. V. Tarasov, A. A. Vladimirov and A. Y. Zharkov, Phys. Lett. B **93** (1980) 429; S. A. Larin and J. A. M. Vermaseren, Phys. Lett. B **303** (1993) 334 [arXiv:hep-ph/9302208].
- [25] M. Misiak and M. Munz, Phys. Lett. B **344** (1995) 308 [arXiv:hep-ph/9409454]; K. G. Chetyrkin, M. Misiak and M. Munz, Nucl. Phys. B **518** (1998) 473 [arXiv:hep-ph/9711266].
- [26] E. Egorian and O. V. Tarasov, Teor. Mat. Fiz. **41** (1979) 26 [Theor. Math. Phys. **41** (1979) 863].
- [27] R. Tarrach, Nucl. Phys. B **183** (1981) 384; D. J. Broadhurst and A. G. Grozin, Phys. Rev. D **52** (1995) 4082 [arXiv:hep-ph/9410240].